ENC 2012
EUROPEAN NUCLEAR CONFERENCE

Transactions Research Reactors

EUROPEAN NUCLEAR SOCIETY

ENS CONFERENCE

ENC 2012 Diamond Sponsor:

HITACHI

ENC 2012 Gold Sponsors:

AGORIA
no future without technology

Belgoprocess

SCK·CEN
STUDIECENTRUM VOOR KERNENERGIE
CENTRE D'ETUDE DE L'ENERGIE NUCLEAIRE

NUCLEAIR FORUM NUCLEAIRE

ENC 2012 Silver Sponsor:

urenco

ENC 2012 Sponsor:

ONET TECHNOLOGIES

organised in collaboration with:

the Nuclear Institute

IAEA International Atomic Energy Agency

NEA Nuclear Energy Agency

European Nuclear Society
Rue Belliard 65
1040 Brussels, Belgium
Phone + 32 2 505 30 54
Fax +32 2 502 39 02
E-mail ens@euronuclear.org
Internet www.euronuclear.org

ISBN 978-92-95064-14-0

These transactions contain all contributions submitted by 7 December 2012.

Page		
5	STEADY STATE THERMAL HYDRAULIC OPERATIONAL PARAMETERS AND SAFETY MARGINS OF NIRR-1 WITH LEU FUEL USING PLTEMP-ANL CODE	Jonah, S. (1); Ibrahim, Y. (1); Kalimullah, M. (2); Matos, J. (2) 1 - Centre for Energy Research and Training, Ahmadu Bello University, P.M.B. 1014, Zaria, Nigeria 2 - Nuclear Engineering Division, Argonne National Laboratory, 9700 S. Cass Avenue, Argonne, IL-60439, United states
13	MYRRHA - A Flexible and Fast Spectrum Irradiation Facility	Baeten, P. (1); Fernandez, R. (1); De bruyn, D. (1); Van den eynde, G. (1); Malambu, E. (1); Aït abderrahim, H. (1) 1 - SCK•CEN, Belgium
22	Absolute Flux Measurement by NAA at the Pavia University TRIGA Mark II reactor facilities	Chiesa, D. (1); Borio di tigliole, A. (2); Cammi, A. (3); Clemenza, M. (1); Nastasi, M. (1); Pattavina, L. (4); Previtali, E. (4); Salvini, A. (2); Sisti, M. (1) 1 - Università degli Studi di Milano Bicocca, Italy 2 - Laboratorio di Energia Nucleare Applicata (L.E.N.A.) Università di Pavia, Italy 3 - Politecnico di Milano, Italy 4 - Istituto Nazionale di Fisica Nucleare sez. Milano Bicocca, Italy
27	Experimental instrumentation for measurement of reactivity temperature and voiding effects at zero power research reactor	Bily, T. (1); Sklenka, L. (1) 1 - Czech Technical University in Prague, Czech republic
34	Design and simulation of the safety systems for a nuclear test facility with supercritical water	Raqué, M. (1); Schulenberg, T. (2) 1 - EnBW Kernkraft GmbH, Germany 2 - Karlsruhe Institute of Technology, Germany

RESEARCH REACTORS

STEADY STATE THERMAL HYDRAULIC OPERATIONAL PARAMETERS AND SAFETY MARGINS OF NIRR-1 WITH LEU FUEL USING PLTEMP-ANL CODE

S.A. JONAH, Y.V. IBRAHIM,

Centre for Energy Research and Training, Ahmadu Bello University,

P.M.B. 1014, Samaru-Zaria, Nigeria

M. KALIMULLAH, J.E. MATOS

Nuclear Engineering Division, RERTR Program. Argonne National Laboratory,

63490, Illinois, USA

ABSTRACT

The PLTEMP/ANL code version 4.1, 2011 was used to perform thermal hydraulic analysis of a miniature neutron source reactor (MNSR) facility with the proposed UO_2 LEU fuel core having 348 fuel pins in the core configuration and at a proposed nominal power of 34 kW for the determination of steady state operational parameters and safety margins. Measured data of NIRR-1 with the current HEU I core at the present nominal power of 31 kW was used to validate calculated data. Results show that the LEU margin to ONB, relative to nominal operating powers of 34 kW is substantially high and compares well with the corresponding margin for HEU core. Considering that the cladding material and the fuel for the proposed LEU core have higher melting points as well as higher resistance to corrosion, the safety margins for steady state operation are enhanced for the conversion of NIRR-1 in particular and MNSR in general.

1. Introduction

The PLTEMP/ANL series of code have been frequently used to perform thermal hydraulic analysis of research reactors for the determination of steady state parameters and safety margins [1]. The steady state parameters include fuel, clad, and coolant temperatures as functions of power. Safety parameters such as peak heat flux, the minimum critical heat flux (CHF), the minimum flow instability power ratio (FIR) and the margin to onset of nucleate boiling (ONB). The code also calculates radial and axial distributions of fuel, cladding, and coolant temperatures in a fuel assembly consisting of several coaxial fuel tubes cooled by light water or heavy water flowing in the annular gaps (i.e. coolant channels) between adjacent fuel tubes. To demonstrate the application of the code for the first time to calculate natural circulation flow rate in a reactor having solid fuels, the Nigeria Research Reactor-1 (NIRR-1) was modeled by the code. NIRR-1 is a Miniature Neutron Source Reactor (MNSR) designed by the China Institute of Atomic Energy (CIAE). The present HEU core of NIRR-1 is made up of 347 fuel pins with an enrichment of over 90 % and three Al dummy rods [2]. A detailed physics description of NIRR-1 has been provided in ref. [3]. Furthermore, neutronics analysis has shown that conversion to

LEU is feasible using UO_2 fuel enriched to 12.5% [4]. A comparison of main parameters of current HEU core and the proposed LEU core of NIRR-1 is given Table 1. In another development, the CIAE has designed and commissioned a variant of the MNSR. It is known as the In-Hospital Neutron Irradiator (IHNI) for boron neutron capture therapy (BNCT) applications and has been designed from scratch to use LEU UO_2 fuel [5]. This paper presents preliminary results of reactor thermal-hydraulic performance and steady state safety analyses for conversion of NIRR-1 from the use of HEU fuel to the use of UO_2 LEU fuel. The objective of this work was to show that it is feasible to use the UO_2 fuel element that could safely replace the current HEU fuel.

	HEU	LEU
Type	Tank-in-pool	Tank-in-pool
Nominal core power (kW_{th})	31	34
Coolant/Moderator	De-ionised light water	De-ionised light water
Loading of U-235 in core (g)	1006.65	1357.86
Reflector	Metallic beryllium	Metallic beryllium
Excess reactivity - cold, clean (mk)	3.77	4.02
Neutron flux at inner irradiation sites	1×10^{12} $cm^{-2}s^{-1}$, stability $\pm$ 1%, horizontal and vertical variation < 3%	1.04×10^{12} $cm^{-2}s^{-1}$, stability $\pm$ 1%, horizontal and vertical variation < 3%
Number of irradiation sites	10 sites (5 inner and 5 outer)	10 sites (5 inner and 5 outer)
Core reactivity temperature coefficient	-0.1 mk/^{o}C; for core temperature 15-40 ^{o}C	-0.1 mk/^{o}C; for core temperature 15-40 ^{o}C

Table 1 A comparison of the main specifications of the HEU core and proposed LEU core of NIRR-1

2. Materials and Method

NIRR-1 is a low-power, tank-in-pool reactor with a nominal thermal power of 30 kW under steady state condition. It is sited at the Centre for Energy Research and Training, Ahmadu Bello University, Zaria, Nigeria and is one of the commercial MNSR facilities. The reactor core is a square cylinder of dimensions 23 cm by 23 cm and it is surrounded by Be annulus on the sides and a Be plate at the bottom. A tray for shimming the reactor in the event of reactivity loss due to Sm poison sits on top of core. The fuel elements are pin types and are arranged in a bird cage, consisting of 350 lattices for the fuel pins. A single control rod made up of Cd material in stainless steel cladding moves centrally inside a guide tube located at the centre of the core.

The whole core configuration sits in light water which serves as both coolant and moderator. The core is designed to be under-moderated with the number of $H/^{235}U$ ratio as 197 for the commercial MNSR. Thermal-hydraulics characteristics of HEU core stems from the use of $U\text{-}Al_4$ as fuel. The fuel type has a low linear power density of about 3.8 W/cm, which is comparable to that of power reactors [6]. The choice of the fuel meat provides a high value of thermal conductivity, while natural convection is adopted for cooling. Figure 1 shows a cartoon of the reactor.

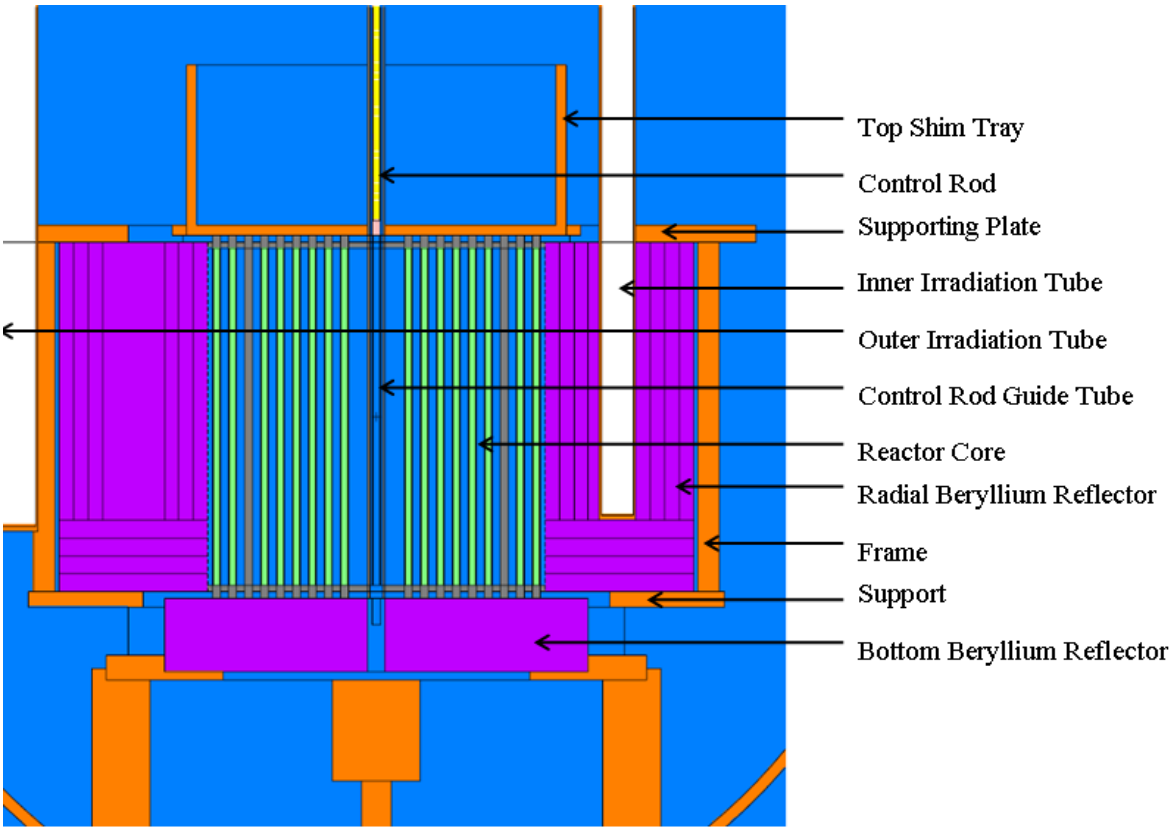

Fig.1 A close Side View of the NIRR-1 HEU Core configuration

PLTEMP/ANL is descended from the original PLTEMP code and was created to obtain a 1-dimensional steady-state temperature solution for a reactor core consisting of a group of nuclear reactor fuel assemblies, each comprised of multiple flat plates separated by coolant channels. The thermal conductivity of a variety of uranium-aluminum alloy fuels can be obtained from interpolation or from fitted equations. A series of calculations could be performed in one run to span a desired range of pressure drops. Some adjustments to the code were made for application to MNSR facilities to calculate the natural circulation flow rates and the code convergence. The number of coolant channels in the fuel assembly is always one more than the number of fuel tubes. This difference is required in the code input data. The innermost boundary of the first channel and the outermost boundary of last channel are assumed to be adiabatic in the multi tube radial heat transfer model of the code. Therefore in order to make use of the

existing provision, an artificial coolant channel of negligible radius (e.g. 1.075 mm) was created in the solid fuel rods used in MNSR facilities as shown in Fig 2. The dimensions of unit cell in Fig.2 are displayed in Table. To improve the code convergence, the outer iteration relaxation factors ε and the inner relaxation factor Finner were made part of the input data via inputs EPSLN and EPSNI on card 500 so that the user could adjust them as needed for convergence. Specific adjustments made in modeling NIRR-1 include the division of the 350 fuel/clad lattices into 24 type of fuel assemblies with 23 of them consisting of 15 fuel pins each and the 24th assembly with 2 or 3 fuel pins respectively for the HEU and LEU cores. Calculations were performed using Bergles-Rohsenow boiling correlation option for water over the pressure range 1-138 bar, which includes the MNSR operating pressure range with the iteration option, ITRNCHF enabled.

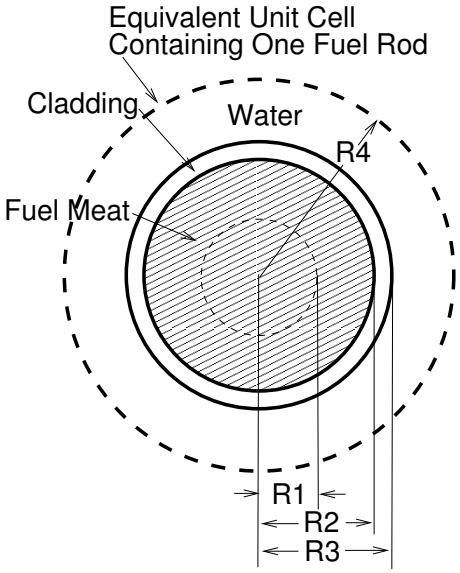

Fig. 2. PLTEMP/ANL Model of NIRR-1 HEU Core Fuel Pin

	Radius, mm
R1	1.075
R2	2.15
R3	2.75
R4	6.2167

Table 2 Dimensions of the unit cell show in Fig. 2

The reactor design data taken from ref. [7] was used in the safety margin calculations and are summarized in Table 3. The power distributions in the HEU and LEU cores of NIRR-1 were calculated using the MCNP5 code. The axial power profiles of the peak and average power fuel pins in the HEU and LEU cores were obtained from neutronics data. The hydraulic resistance of the coolant flow circuit in the PLTEMP/ANL model was obtained by calibrating the model to reproduce an experimentally measured coolant temperature rise of 13 ℃ (from 24.5 ℃ to 37.5 ℃) at a reactor power of 15 kW from measurements [8]. The results of this calibration for both reactor cores are also given in Table 3. Using the calibrated model, the coolant inlet temperature was raised and adjusted to get an outlet temperature of 70 ℃ in steady-state at the nominal reactor power. Table 3 also shows the adjusted inlet temperature and some operating parameters found by this calculation

3. Results and Discussion

Results in Table 4 show that measured data for current HEU core compare well with calculated data obtained by the PLTEMP code. Data are presented for operation at full powers, 31 kW and 34 kW respectfully for the current HEU core and the proposed LEU core. The calculated thermal hydraulic steady state operational characteristics and safety margins for NIRR-1 with the proposed UO_2 LEU fuel in the Table compare well with HEU data. The power at which ONB occur has been examined for the LEU fuel configuration and compared with the corresponding margins for the HEU fuel configuration. The results obtained were deemed more conservative and can be seen in the Table. The power level at which ONB occurs was calculated to be 65.2 kW and 67.8 kW respectively for the HEU and LEU cores. As can be seen, the prediction is far above the maximum operating power levels for the two cores. The maximum temperature of 113.2 ℃ at the surface of the zircaloy cladding for the LEU fuel is far below its melting temperature of 1850 ℃. Similarly, the maximum temperature of 147 ℃ at the fuel centerline is far below the melting temperature of 2865 ℃ for UO_2 fuel. At power levels above ONB, calculations have shown that the reactor would operate in the sub-cooled boiling regime until Onset of Significant Void (OSV) occurs at a power level of ~ 145 kW. The critical heat flux (CHF) would be reached at a power level far above that at which OSV is predicted to occur. Overall, these analyses show that the steady state thermal-hydraulics safety margins for the proposed LEU design compare with the HEU data and still satisfy technical specifications. Considering that the UO2 fuel and zircaloy clad have higher melting points and better resistance to corrosion compared with the materials of the current HEU core.

Thermal-Hydraulic Data	HEU	LEU
Reactor Power	31	34
Number of Fuel Pins in Reactor	347	348
Peak Pin Power, W	99.66	113.19
Average Pin Power, W	86.96	97.70
Peak Pin/Average Pin Power Ratio	1.146 ±0.3%	1.1586 ±0.3%
Fuel Meat	U-Al alloy	UO_2
Uranium enrichment	90.2 %	12.5 %
Cladding Material	Al alloy	Zircaloy-4
Gas in Meat-Cladding Gap	-	He
Meat Radius, mm	2.15	2.15
Gas Gap Thickness, mm	-	0.05
Cladding Thickness, mm	0.6	0.6
Fueled Length, m	0.230	0.230
Unheated Length Below the Fueled Length, m	0.009	0.009
Unheated Length Above the Fueled Length, m	0.009	0.009
Total Height of a Fuel Pin, mm	0.248	0.248
Inner Diameter of Annular Beryllium Around All Fuel Pins, m	0.231	0.231
Fuel Meat Thermal Cond., W/m-C	140	5.78
Cladding Thermal Cond., W/m-C	180	14.74
Gap Gas Thermal Cond., W/m-C	-	0.1767
Gap Thermal Resistance, m^2-C/W	-	~ 0.000283
Hydraulic Diameter for Hot Pin, m	0.0231	0.0231
Flow Area for Hot Pin, m^2	9.978E-5	9.978E-5
Depth of Water Above Core Top, m	4.7	4.7
Pressure at Core Top, MPa	0.1468	0.1468
Calibration of Hydraulic Loss Based on a Test at 15 kW:		
Core Inlet Temperature, ℃	24.5	24.5
Coolant Temp. Rise, ℃	13	13
Calibrated Loss Coefficient	67.3	68.6
Calculated Core Flow Rate, kg/s	0.277	0.277
Steady-State at Nominal Reactor Power with Core Inlet Temp. Adjusted to Get an Exit Temp. of 70 ℃:		
Adjusted Inlet Temperature, ℃	53.78	52.28
Core Flow Rate, kg/s	0.441	0.47
Coolant Outlet Temperature, ℃	70.0	70.0
Max. Cladding Surface Temp., ℃	86.4	87.8
Max. Fuel Centerline Temp., ℃	86.7	100.5

Table 3 Thermal Hydraulic Analysis of NIRR-1 Using PLTEMP/ANL Code

Parameters	HEU Core at 31 kW		LEU Core at 34 kW
	Measured	PLTEMP	PLTEMP
T_{out} (^oC)	45.2	44.13	36.93
T_{clad} (^oC)	-	112.7	112.7
Reactor Power at ONBR=1 on Peak Pin Without Hot Channel Factors	-	65.2	67.8
CORE FLOW (Kg/s)	-	0.586	0.586

Table 4 Comparison of Measured and Calculated Steady State T-H Data and Safety Margins for NIRR-1

4. **Conclusion**

A PLTEMP/ANL model of the current HEU core configuration of NIRR-1 was developed to perform the analyses of the thermal-hydraulic characteristics of the reactor operating at steady state. Calculated for the present HEU core obtained agree well with measurements from the SAR [2]. Consequently, the HEU core was replaced with the proposed UO_2 LEU core in order to evaluate the impact of conversion on the steady state thermal hydraulic safety margins. Data obtained show that the maximum cladding surface temperature, centre line temperature and the margins to ONB of the LEU fuel agree well with the corresponding values for the HEU core. The results show that the LEU margin to ONB, relative to nominal operating powers of 34 kW is substantially high and compares well with the corresponding margin for HEU core. Similarly, the predicted clad surface and fuel temperatures for the proposed LEU cores are comparable with the corresponding data for the HEU core. Considering that the cladding material and the fuel for the proposed LEU core have higher melting points as well as higher resistance to corrosion, the safety margins for steady state operation are enhanced for the conversion of NIRR-1 in particular and MNSR in general.

5. Acknowledgements

This work was supported by the IAEA Coordinated Research Project No.NIR/13934 entitled “Conversion of MNSR from HEU to LEU” and Research Agreement, Contract No 1F-30204 UCHICAGO ARGONNE, LLC (Operator of Argonne National Laboratory)

6. References

1. A. P. Olson and M. Kalimullah, "A Users Guide to the PLTEMP/ANL V4.1 Code," Global Threat Reduction Initiative (GTRI) – Conversion Program, Nuclear Engineering Division, Argonne National Laboratory, Chicago, IL, USA (April 5, 2011).
2. Nigeria Research Reactor-1: Final Safety Analysis Report, Centre for Energy Research and Training, Energy Commission of Nigeria, Ahmadu Bello University, Zaria, CERT/NIRR-1/001, August 2005.
3. Jonah S.A., Liaw J.R., Matos J.E., 2007. Monte Carlo simulation of core physics parameters of the Nigeria Research Reactor-1(NIRR-1)" Annals Nucl. Energy 34, 953-957
4. Jonah S. A., Ibikunle K., Li Yi-guo. "A feasibility study of LEU enrichment uranium fuels for MNSR conversion using MCNP" Annals of Nuclear Energy, 36 (2009), 1285 –1286
5. Li Yi-guo, "The Physics Experimental Study for In-Hospital Neutron Irradiator (INHI)", Proc. International Meeting on Reduced Enrichment for Research and Test Reactors, Prague, Czech Republic, 23-27 September 2007
6. Shi Shuangkai, "MNSR Thermal Hydraulics", part of MNSR Training Manual, p. 10, China Institute of Atomic Energy, unpublished, 1993.
7. Ampomah-Amoako E., Akaho E. H. K., Anim-Sampong S., Nyarko B.J.B., "Transient Analysis of Ghana Research Reactor-1 using PARET/ANL Thermal Hydraulic Code," Nucl. Eng. and Design, Vol. 239, pp. 2479-2483 (2009)
8. Ahmed Y.A., Balogun G.I., Jonah S. A., Funtua I. I., "The Behavior of Reactor Power and Flux Resulting from Changes in Core-Coolant Temperature for a Miniature Neutron Source Reactor," Annals of Nuclear Energy, Vol. 35, pp. 2417-2419 (2008).

MYRRHA
A FLEXIBLE AND FAST SPECTRUM IRRADIATION FACILITY

P. BAETEN, R. FERNANDEZ, D. DE BRUYN, G. VAN DEN EYNDE, E. MALAMBU, H. AÏT ABDERRAHIM
Belgian Nuclear Research Centre (SCK•CEN)
Boeretang 200, 2400 Mol (Belgium)

ABSTRACT

Since 1998, SCK•CEN is developing a multipurpose irradiation facility in order to support research programs on fission and fusion reactor structural materials and nuclear fuel development. MYRRHA (Multi-purpose hYbrid Research Reactor for High-tech Applications) is a flexible experimental accelerator driven system (ADS) which is able to work in both subcritical and critical mode.

The objectives of this new research reactor are the demonstration of the ADS concept at a reasonable power level on one hand and to prove the technical feasibility of transmutation of minor actinides and long-lived fission products on the other hand.

In the context of the FP7 Central Design Team (CDT) project, SCK•CEN worked, together with 18 European partners, on the design of a 'Fast Spectrum Transmutation Experimental Facility' (FASTEF). The CDT project finished end March 2012. The design of the MYRRHA reactor at the end of the CDT project is discussed in this paper.

1. INTRODUCTION

Since its creation in 1952, the Belgian Nuclear Research Centre (SCK•CEN) at Mol has always been heavily involved in conception, design, realisation and operation of large nuclear infrastructures. The Centre has even played a pioneering role in such type of infrastructures in Europe and worldwide. SCK•CEN has successfully operated these facilities at all times thanks to the high degree of qualification and competence of its personnel and by inserting these facilities in European and international research networks, contributing to the development of crucial aspects of nuclear energy at international level.

One of the flagships of the nuclear infrastructure of SCK•CEN is the BR2 reactor, a flexible irradiation facility known as a multipurpose materials testing reactor (MTR). This reactor is in operation since 1962 and has proven to be an excellent research tool, which has produced remarkable results for the international nuclear energy community in various fields such as material research for fission and fusion reactors, fuel research, reactor safety, reactor technology and for the production of radioisotopes for medical and industrial applications. BR2 has been refurbished twice, consisting of the replacement of the beryllium matrix and considerable safety improvements, in the beginning of the eighties and in the mid-nineties.

The BR2 reactor is now licensed for operating until 2016 with a potential extension for another ten-year period until 2026. The SCK•CEN at Mol is working since several years at the pre- and conceptual design of a multi-purpose flexible irradiation facility, that can replace BR2 and that is innovative to support long-term oriented research projects ensuring the future of our research centre. This facility, called MYRRHA[1], has been designed as a multipurpose Accelerator Driven System (ADS) for R&D applications, and consists of a proton accelerator delivering its beam to a spallation target that in turn couples to a sub-critical fast core, cooled with Lead-Bismuth Eutectic (LBE).

To determine the characteristics of this multi-purpose flexible irradiation facility, an analysis of the present day needs of the international community has been conducted in particular in the European Union and as a conclusion, MYRRHA should target the following applications catalogue:

- To demonstrate the ADS full concept by coupling the three components (accelerator, spallation target and sub-critical reactor) at reasonable power level to allow operation feedback, scalable to an industrial demonstrator.

- To allow study of the efficient transmutation of high-level nuclear waste, in particular minor actinides that would request high fast flux intensity ($\Phi_{>0.75MeV}$ = 10^{15} n.cm^{-2}.s^{-1}),
- To be operated as a flexible fast spectrum irradiation facility allowing (a) for fuel developments for innovative reactor systems, (b) for material developments for GEN IV systems and for fusion reactors and finally (c) for radioisotope production for medical and industrial applications (holding a backup role for classical medical radioisotopes and focusing on R&D and production of radioisotopes requesting very high thermal flux levels).

The different versions of MYRRHA have been included in successive collaborative projects of the European Commission in its framework programmes. In particular the 2005 version has been offered as a starting basis for the XT-ADS design within the EUROTRANS project (2005-2010)[2] in the 6th framework programme in the context of Partitioning and Transmutation.

XT-ADS was intended as a short-term (operational around 2020) small-scale (50 to 100 MW_{th}) experimental facility that should demonstrate the technical feasibility of transmutation in an ADS. At the end of the EUROTRANS project, the XT-ADS design has complied with the project main requirements. Nevertheless, some technical solutions for achieving them still remained to be confirmed.

Within this paper, an overall view of the MYRRHA project at its current state is described. Section 2 describes the linear accelerator used for MYRRHA. Section 3 handles about the current design of the MYRRHA core and primary system. Section 4 is devoted to the reactor building design and plant layout. At last, section 5 is describing the further developments still under considerations.

2. THE MYRRHA ACCELERATOR

The accelerator is the driver of MYRRHA since it provides the high energy protons that are used in the spallation target to create neutrons which in turn feed the subcritical core. In the current design of MYRRHA, the machine must be able to provide a proton beam with an energy of 600 MeV and an average beam current of 3.2 mA. The beam is delivered to the core in continuous wave (CW) mode. Once a second, the beam is shut off for 200 µs so that accurate on-line measurements and monitoring of the sub-criticality of the reactor can take place. The beam is delivered to the core from above through a beam window.

Accelerator availability is a crucial issue for the operation of the ADS. A high availability is expressed by a long Mean Time Between Failure (MTBF), which is commonly obtained by a combination of over-design and redundancy. On top of these two strategies, fault tolerance must be implemented to obtain the required MTBF. Fault tolerance will allow the accelerator to recover the beam within a beam trip duration tolerance after failure of a single component. In the MYRRHA case, the beam trip duration tolerance is 3 seconds. Within an operational period of MYRRHA the number of allowed beam trips exceeding 3 seconds must remain under 10, shorter beam trips are allowed without limitations. The combination of redundancy and fault tolerance should allow obtaining a MTBF value in excess of 250 hours.

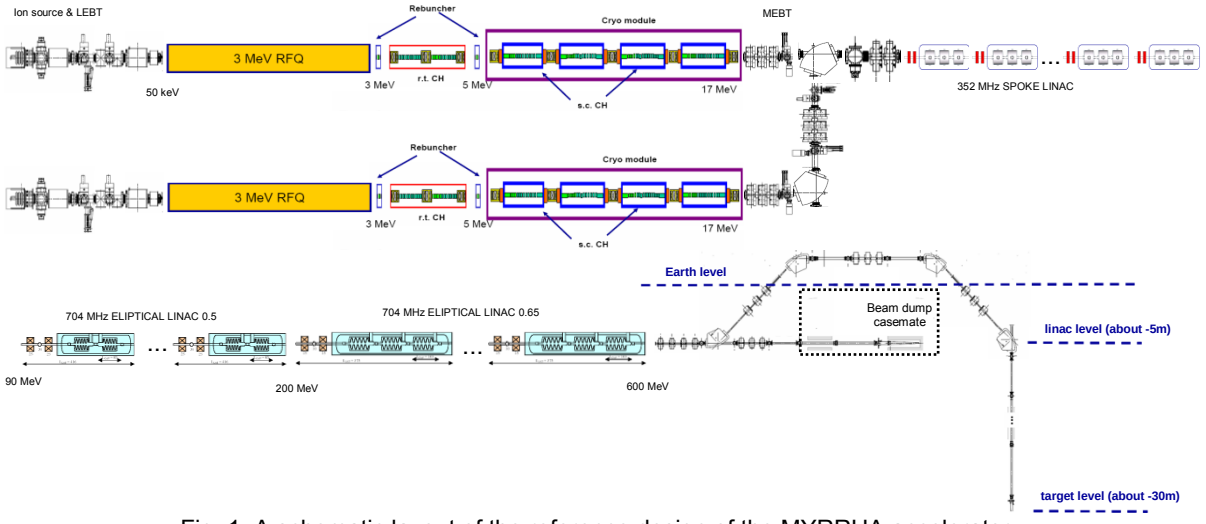

Fig. 1: A schematic layout of the reference design of the MYRRHA accelerator.

At present proton accelerators with megawatt level beam power in CW mode only exist in two basic concepts: sector-focused cyclotrons and linear accelerators (linacs). Cyclotrons are an attractive

option with respect to construction costs, but they don't have any modularity which means that a fault tolerance scheme cannot be implemented. Also, an upgrade of its beam energy is not a realistic option. A linear accelerator, especially if made superconducting, has the potential for implementing a fault tolerance scheme and offers a high modularity, resulting in the possibility to recover the beam within a short time and increasing the beam energy.

A basic layout of the MYRRHA accelerator, aiming at maximizing its efficiency, its reliability (or MTBF) and its modularity, is provided in Fig. 1.

3. DESIGN OF THE CORE AND PRIMARY SYSTEM OF MYRRHA

The main components/systems of the current MYRRHA-FASTEF design are of the same MYRRHA/XT-ADS type, as defined within the EUROTRANS project, with only increased size. The primary and secondary systems have been designed to evacuate a maximum core power of 100 MW_{th}. All the MYRRHA-FASTEF components are optimized for the extensive use of the remote handling system during components replacement, inspection and handling.

Since MYRRHA-FASTEF is a pool-type ADS, the reactor vessel houses all the primary systems. In previous designs of MYRRHA, an outer vessel served as secondary containment in case the reactor vessel leaks or breaks. In the current design, the reactor pit implements this function, improving the capabilities of the reactor vault air cooling system. The vessel is closed by the reactor cover which supports all the in-vessel components. A diaphragm inside the vessel functions to separate the hot and cold LBE, to support the IVFS and to provide a pressure separation. The core is held in place by the core support structure consisting of a core barrel and a core support plate. Fig. 2 shows a section of the MYRRHA-FASTEF reactor showing its main internal components.

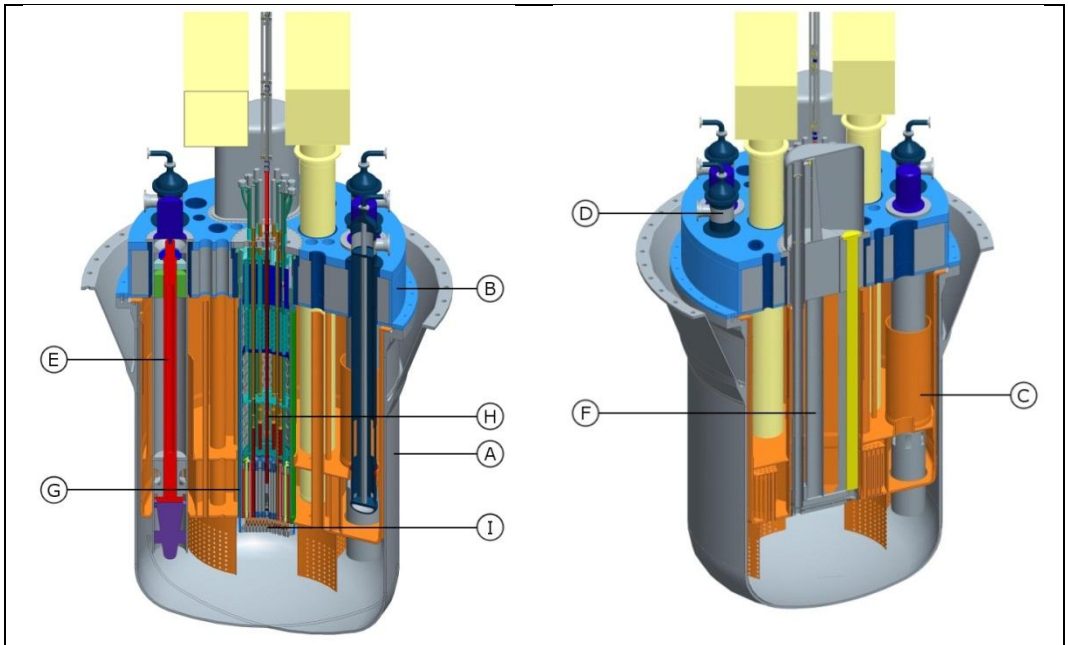

Fig. 2: Section of the MYRRHA-FASTEF reactor

At the present state of the design, the reactor core (Fig. 3) consists of mixed oxide (MOX) fuel pins, typical for fast reactors. A major change with respect to the previous version of the core is the switch from a windowless loop-type spallation target to a windowed beam tube-type spallation target. The previous version needed three central hexagons to house the spallation target while the present day design only needs one central hexagon. To better accommodate this central target, the fuel assemblies size is a little bit increased as compared to the MYRRHA/XT-ADS design. Consequently the In-Pile test Sections (IPS), which will be located in dedicated FAs positions, are larger in diameter giving more flexibility for experiments. Thirty seven positions can be occupied by IPSs or by the spallation target (the central one of the core in sub-critical configuration) or by control and shutdown

rods (in the core critical configuration). This gives a large flexibility in the choice of the more suitable position (neutron flux) for each experiment.

The requested high fast flux intensity has been obtained optimizing the core configuration geometry (fuel rod diameter and pitch) and maximizing the power density. We will be using, for the first core loadings, 15-15Ti as cladding material instead of T91 that will be qualified progressively further on during MYRRHA operation. The use of lead-bismuth eutectic (LBE) as coolant permits to lower the core inlet operating temperature (down to 270 °C) decreasing the risk of corrosion and allowing to increase the core ΔT. This together with the adoption of reliable and passive shutdown systems will permit to meet the high fast flux intensity target.

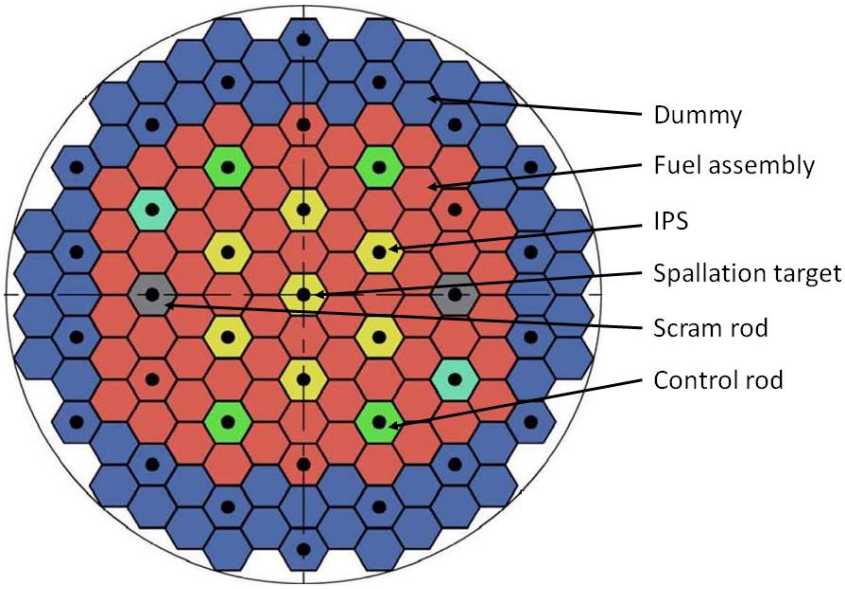

Fig. 3: Cut in the MYRRHA-FASTEF core,
showing the central target, the different types of fuel assemblies and dummy components.

As depicted in Fig. 3, showing a critical core layout (with 7 central IPS) at the equilibrium of the fuel cycle, 37 positions are available for Multi-Functional Channels (MFC) that can host indifferently:

- fuel assembly and dummy, loaded from the bottom (in all the 151 positions);
- IPS, control and scram rods, loaded from the top.

In subcritical mode the accelerator (as described in the previous section) is the driver of the system. It provides the high energy protons that are used in the spallation target to create neutrons which in their turn feed the subcritical core. The accelerator is able to provide a proton beam with energy of 600 MeV and a maximum current of 4 mA.

In subcritical mode the spallation target assembly, located in the central position of the core, brings the proton beam via the beam tube into the central core region. The assembly evacuates the spallation heat deposit, guarantees the barrier between the LBE and the reactor hall and assures optimal conditions for the spallation reaction. The assembly is conceived as an IPS and is easily removable or replaceable.

Differently from the critical layout (Fig. 3), in ADS mode the six control rods (buoyancy driven in LBE) and the three scram rods (gravity driven in LBE) will be replaced by absorbing devices to be adopted only during refuelling. Thanks to the (aimed and reached) flexibility, such absorbing devices will be implemented by adopting the Control Rods, but they will be controlled manually only by the operator.

The primary, secondary and tertiary cooling systems have been designed to evacuate a maximum thermal core power of 110 MW. The 10 MW more than the nominal core power account for the power deposited by the protons, for the power of in-vessel fuel and for the power deposited in the structures by γ-heating. The average coolant temperature increase in the core in nominal conditions is 140 °C with a coolant velocity of 2 m/s. The primary cooling system consists of two pumps and four primary heat exchangers (PHX).

The primary pumps shall deliver the LBE to the core with a mass flow rate of 4750 kg/s (453 l/s per pump). The working pressure of the pump is 300 kPa. The pump will be fixed at the top of the reactor cover, which is supposed to be the only supporting and guiding element of the pump assembly.

The secondary cooling system is a water cooling system while the tertiary system is an air cooling system. These systems function in active mode during normal operation and in passive mode in emergency conditions for decay heat removal.

The main thermal connection between the primary and secondary cooling systems is provided by the primary heat exchangers (Fig. 4). These heat exchangers are shell and tube, single-pass and counter-current heat exchangers. Pressurized water at 200 °C is used as secondary coolant, flowing through the feed-water pipe in the centre of the PHX to the lower dome. All the walls separating the LBE and water plena (feed-water tube, lower dome and upper annular space) are double walled to avoid pre-heating of the secondary coolant and to prevent water leaking in the LBE in case of tube failure.

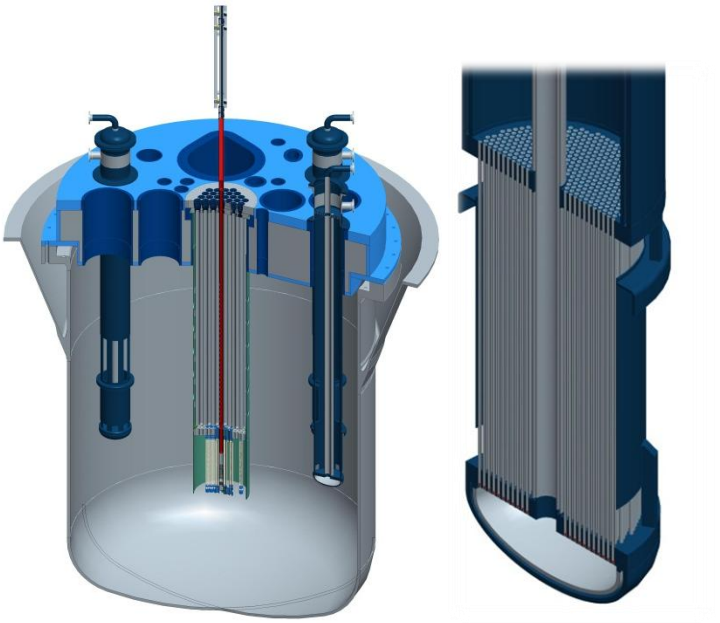

Fig. 4: Heat Exchangers

In case of loss of the primary flow (primary pumps failure), the primary heat exchangers aren't able to extract the full heat power. In such cases, the beam must be shut off in the subcritical case and the shutdown rods inserted in the critical case. The decay heat removal (DHR) is achieved by natural convection. Ultimate DHR is done through the reactor vessel coolant system (RVACS, reactor vessel air cooling system) by natural convection.

The interference of the core with the proton beam, the fact that the room situated directly above the core will be occupied by lots of instrumentation and IPS penetrations, and core compactness result in insufficient space for fuel handling to (un)load the core from above. Since the very first design of MYRRHA, fuel handling is performed from underneath the core. Fuel assemblies are kept by buoyancy under the core support plate.

Two fuel handling machines are used, located at opposite sides of the core. Each machine covers one side of the core. The use of two machines provides sufficient range to cover the necessary fuel storage positions without the need of an increase for the reactor vessel when only one fuel handling machine is used. Each machine is based on the well-known fast reactor technology of the 'rotating plug' concept using SCARA (Selective Compliant Assembly Robot Arm) robots. To extract or insert the fuel assemblies, the robot arm can move up or down for about 2 meters. A gripper and guide arm is used to handle the FAs: the gripper locks the FA and the guide has two functions, namely to hold the FA in the vertical orientation and to ensure neighbouring FAs are not disturbed when a FA is extracted from the core. An ultrasonic (US) sensor is used to uniquely identify the FAs.

The in-vessel fuel handling machine will also perform in-vessel inspection and recovery of an unconstrained FA. Incremental single-point scanning of the diaphragm can be performed by an US sensor mounted at the gripper of the IVFHM. The baffle under the diaphragm is crucial of the strategy as it limits the work area where inspection and recovery are needed. It eliminates also the need of additional recovery and inspection manipulators, prevents items from migrating into the space between the diaphragm and the reactor cover, and permits side scanning.

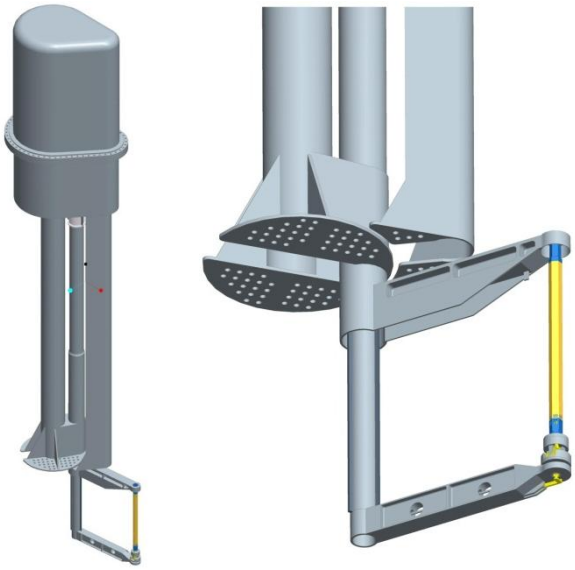

Fig. 5: The in-vessel fuel handling machine

4. REACTOR BUILDING DESIGN AND PLANT LAYOUT

The work described in this section deals with the so-called balance of plant studies, in other words all elements in the FASTEF facility outside the reactor vessel and its internals. One of the first activities was to determine the requirements for the reactor building (dimensions, configuration, containment, etc.), fuel handling (fresh and spent), radiological safety and infrastructure, auxiliary systems, instrumentation and, finally, the general layout of the whole plant on the technical site of SCK•CEN.

When determining the criteria for the plant, it should be recalled that the FASTEF reactor has a power of 100 MW_{th} (much larger than the XT-ADS concept in the FP6 EUROTRANS project), cooled by LBE, capable of operating in critical or subcritical mode and to which a 600 MeV linear accelerator (LINAC) is attached. In addition, the reactor must be able to carry out experiments on irradiating materials, doping silicon ingots, producing medical radioisotopes and others so as to endow the facility with great versatility but on the other hand making it extremely complex.

Fig. 6: The present FASTEF facility within the existing installations

The plant comprises a reactor building, a LINAC tunnel, an accelerator front-end building, control buildings, a spent fuel storage building and other auxiliary buildings needed for plant services.

To reduce costs and facilitate the construction process, the LINAC tunnel is at the ground level and afterwards covered by a 7 m thick sand layer to enhance radiological protection. All buildings of the plant are constructed above ground, except for the reactor building where the reactor vessel and reactor cover lie completely under ground level. This is an important difference with the previous development in the EUROTRANS project. Fig. 6 presents the layout of the FASTEF facility within the existing installations on the SCK•CEN technical site.

An important point in this general layout is that the FASTEF buildings are aligned with the overall grid present on the SCK•CEN site to obtain an easy and effective relation to the existing buildings and infrastructure. The minimum distance between buildings depends on the fire prevention regulations and also takes into account the accessibility of the buildings. The fixed junction of the front-end building, the LINAC tunnel and the reactor building, which add up to a total length of approximately 400 m determine a large part of the general layout. Room for future extensions, either for MYRRHA or for other SCK•CEN projects, has also been foreseen.

The design of the reactor building started off with the reactor hall (taken from the XT-ADS facility – a rectangle of 40 m length by 16 m width) at the centre and enlarging from there by implementing the related rooms. When developing the reactor hall, the main philosophy was to ensure that the clean zones remained clean. This was achieved by determining that the movement of any elements was only done in one direction: new elements only entered through a dedicated airlock, and the same criterion was applied for bringing in fresh fuel, taking out waste, spent fuel and experiments. In addition to these requirements, one element that has seriously influenced the design is the vacuum line, which also must be removable, connecting the accelerator to the reactor. The design of the ventilation system considers the strict requirements of the reactor hall atmosphere (nitrogen at an underpressure of 350 Pa). The accelerator line is laid perpendicular to the vertical axis of the reactor, thereby making it necessary to place electro-magnets to bend the beam: two at 45 degrees and one at 90 degrees (see Fig. 7).

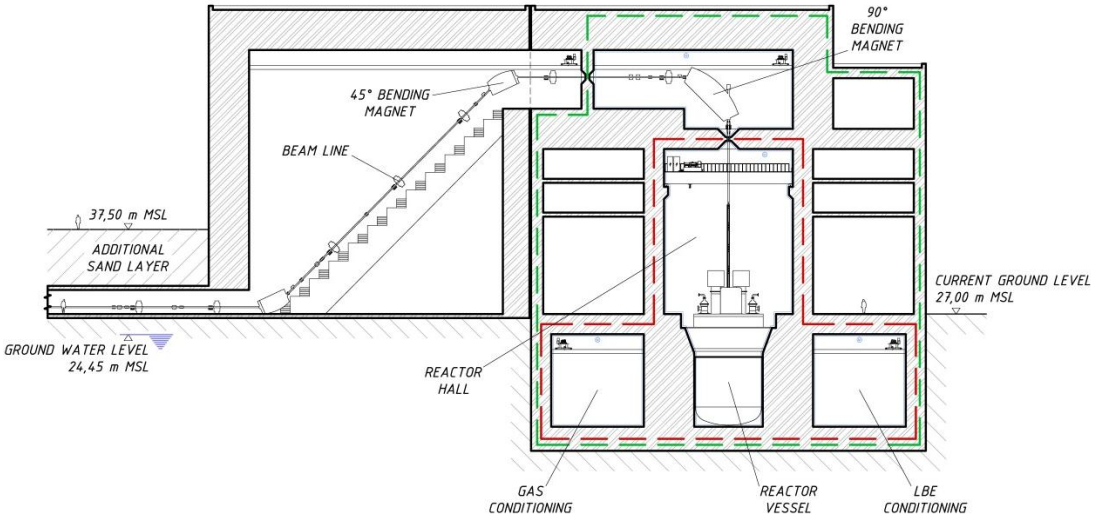

Fig. 7: Vertical cross-section in the reactor building, showing the beam line entry in the reactor vessel

Once the position of the reactor within the reactor hall has been set, the space requirements are determined for the reactor hall. Study was made of the movement of new elements, waste and space for maintenance in the reactor hall. The width of the reactor hall was determined based on the maximum extension of a proved technology remote handling system while the height was determined by the length of the longest equipment inside the reactor (the heat exchanger), the reactor hall crane (200 t) and the accelerator vacuum line. It was decided to provide a storage pit inside the reactor hall to foresee the possible substitution of the reactor lid and of the diaphragm during the plant lifetime. This allows designing the airlocks, entrances, exits and doors for operational modes and not for the size of these two very large components.

With the current building configuration the first seismic response spectra in the main equipment locations have been calculated. Our safety approach comprises two levels of seismic loading: the design- and beyond design-based earthquakes. Special attention to the seismic calculations is the consequence of the Fukushima accident.

The current FASTEF reactor building layout is larger than in the previous XT-ADS concept, but many functions foreseen in separate buildings are now concentrated in one single building with easier

material and personnel workflows. Still, civil engineering represents between 25 and 30 percent of the total investment costs of the project, what justifies the past and current iterations.

5. FURTHER R&D DEVELOPMENTS

In the following years, a lot of R&D must be performed in order to support the design work and the safety analysis of the facility presented in this paper.

First of all, it is essential to perform the necessary R&D to support the qualification of the MOX fast driver fuel and the investigation of structural and cladding material behaviour in reactor conditions.

Then, the main goal of the material R&D and qualification programme is to provide reliable material property data for the design and licensing of FASTEF. Within the MYRRHA project as a whole, it is preferred to consider industrially available and qualified materials, rather than to develop and optimize new materials. Based on the available material properties, 15-15Ti, T91 and 316L have been selected as the candidate materials. Austenitic stainless steels, including 15-15Ti and 316L, have been used in the construction of fast, sodium-cooled, reactors and are well characterized for nuclear applications. However, due to the innovative character of FASTEF, further investigation on the material behaviour and performances must be done. On this moment, four overlapping activities regarding material R&D are performed: a) identification of the material issues for design and licensing, b) development of test and evaluation guidelines for structural materials characterisation, c) assessment of material properties and finally d) development of testing infrastructure.

Finally, for a long-term operation of a LBE cooled facility, chemistry control and monitoring is crucial for the reactor. LBE chemistry and conditioning R&D programme handles about the LBE technology related to the chemical control of the coolant and the purification of the evaporated gasses. Several issues have been identified for this programme: a) development of oxygen sensors to measure the dissolved oxygen concentration in the coolant, b) conditioning of the LBE to minimize dissolution of structural materials and core internals and to prevent formation and precipitation of oxides, c) filtration and trapping of impurities in the LBE, d) evaporation and capture of volatile and/or highly radiotoxic elements from the cover gas and finally e) removal of LBE or dissolved constituents from among others components and test samples.

6. CONCLUSIONS

SCK•CEN is proposing to replace its ageing flagship facility, the Material Testing Reactor BR2, by a new flexible irradiation facility, MYRRHA. Considering the international and European needs, MYRRHA is conceived as a flexible fast spectrum irradiation facility able to work in both sub-critical and critical mode.

MYRRHA is now foreseen to be in full operation by 2024 and it will be able to be operated in both operation modes: subcritical and critical. In subcritical mode, it will demonstrate the ADS technology and the efficient demonstration of MA in sub-critical mode. As a fast spectrum irradiation facility, it will address fuel research for innovative reactor systems, material research for GEN IV systems and for fusion reactors, radioisotope production for medical and industrial applications and industrial applications, such as Si-doping.

The MYRRHA design has now, with the FASTEF version, entered into the Front End Engineering Phase covering the period 2012-2014. The engineering company which will handle this phase is currently being selected. At the end of this phase, the purpose is to have progressed in such a way in the design of the facility that the specifications for the different procurement packages of the facility can be written, to have adequately addressed the remaining outstanding R&D issues, to have obtained the construction and exploitation permits and to have formed the international members' consortium for MYRRHA.

ACKNOWLEDGEMENTS

The XT ADS design work has been performed under the Integrated Project EUROTRANS (Ref. FI6W-CT-2004-516520) cofunded by the European Union in its 6th Framework Programme. The FASTEF design work is being performed under the Collaborative Project CDT (Ref. FP7-232527) cofunded by the European Union in its 7th Framework Programme. Acknowledgment is also due to all the colleagues of the participant institutes for their contributions in many different topics associated with the XT ADS and FASTEF design and operation.

LIST OF ACRONYMS

ADS	Accelerator Driven System
APPM	Atomic Part Per Million
CDT	Central Design Team
CW	Continuous Wave
DHR	Decay Heat Removal
DPA	Displacement Per Atom
FA	Fuel Assembly
FASTEF	Fast Spectrum Transmutation Experimental Facility
FP7	Seventh Framework Programme (of the European Commission)
HLW	High-level Long-lived radioactive Waste
IPS	In-Pile test Section
ISOL	Isotope Separator On-Line
IVHFM	In-vessel Fuel Handling Machine
LBE	Lead-Bismuth Eutectic
LFR	Lead-cooled Fast Reactor
LINAC	Linear Accelerator
LLFP	Long-Lived Fission Products
MA	Minor Actinide
MOX	Mixed Oxide
MTR	Material Testing Reactor
P&T	Partitioning and Transmutation
PHX	Primary Heat Exchanger
PWR	Pressurized Water Reactor
RIB	Radioactive Ion Beams
SCARA	Selective Compliant Assembly Robot Arm or Selective Compliant Articulated Robot Arm
US	Ultrasonic
XT-ADS	eXperimental demonstration of the technical feasibility of Transmutation in an Accelerator Driven System

REFERENCES

[1] H. AÏT ABDERRAHIM & P. BAETEN, “MYRRHA, a Multi-purpose hYbrid Research Reactor for High-tech Applications “, *Proc. Int. Conference PHYSOR 2012 – Advances in Reactor Physics – Linking Research, Industry, and Education*, Knoxville, Tennessee, April 15-20, 2012, American Nuclear Society (2012) (CD-ROM).

[2] D. DE BRUYN, S. LARMIGNAT, A. WOAYE HUNE, L. MANSANI, G. RIMPAULT & C. ARTIOLI, "Accelerator Driven Systems for Transmutation: Main Design Achievements of the XT-ADS and EFIT Systems within the FP6 IP-EUROTRANS Integrated Project", *Proc. Int. Congress on Advances in Nuclear Power Plants* (ICAPP '10), San Diego, California, June 13-17, 2010, American Nuclear Society (2010) (CD-ROM).

ABSOLUTE FLUX MEASUREMENT BY NAA AT THE PAVIA UNIVERSITY TRIGA MARK II REACTOR FACILITIES

A. BORIO DI TIGLIOLE[(1)], A. CAMMI[(2,4)], D. CHIESA[(3)], M. CLEMENZA[(3)], M.NASTASI[(3)], L. PATTAVINA[(4)], E. PREVITALI[(3,4)], A.SALVINI[(1)], M.SISTI[(3)]

(1) University of Pavia, Laboratory of Applied Nuclear Energy, Via Aselli 41, 27100 Pavia, Italy
(2) Polytechnic of Milano, Department of Energy, Via La Masa 34, 20156 Milano, Italy
(3) University of Milano-Bicocca, Physics Department, Piazza della Scienza 3, 20126, Milano, Italy
(4) INFN section of Milano-Bicocca, Piazza della Scienza 3, 20126, Milano, Italy

ABSTRACT

The neutron flux is a crucial parameter to know in the analysis of a nuclear reactor, because it affects the reaction rate and thus the fuel burnup. Moreover, a very precise knowledge of the flux in the irradiation facilities is helpful for benchmarking the simulation models of the reactor. In this paper, we present the results of the measurements of the neutron flux in three irradiation facilities of the TRIGA Mark II reactor installed at the University of Pavia. The neutron activation analysis of samples containing a large number of elements was used to perform an absolute measurement of the flux. The γ-ray spectroscopy measurements were repeated on different HPGe detectors and GEANT4 Monte Carlo simulations were developed to evaluate the detection efficiency for every radioisotope of interest. The very good agreement among the results of the flux calculations from the many different activated isotopes confirms the reliability of the methodology.

1. Introduction

TRIGA reactor description The TRIGA (Training Research and Isotope production General Atomics) Mark II is a pool-type research reactor moderated and cooled by light water. Fuel consists of a uniform mixture of uranium (8%wt, enriched at 20%wt in ^{235}U), hydrogen (1%wt) and zirconium (91%wt). The TRIGA reactor of the University of Pavia has a nominal power of 250 kW in a stationary-state operation. The core shape is a right cylinder and the volume can host up to 90 locations distributed according to 6 concentric rings. These locations can be filled either with fuel elements or different core components like dummy elements (i.e. graphite elements), control rods, neutron sources and irradiation channels. The active dimensions of the core are 45.7 cm in diameter and 35.6 cm in height. A 30 cm thick radial graphite reflector surrounds the core while the axial reflector is provided by the fuel element itself in which two 10 cm thick graphite cylinders are located at the ends of the rod. The TRIGA Mark II reactor in Pavia is equipped with some irradiation facilities. Among them, two are located inside the core: the central thimble, that is an aluminum pipe 3.8 cm in diameter located at the center of the fuel rings, and the pneumatic irradiation system, named "Rabbit", in the outer ring. Recently, a new irradiation facility, named Thermal Channel, was added in the pool just outside the graphite reflector.

Flux measurement by NAA The neutron activation analysis for the evaluation of the flux consists in irradiating some samples with a known amount of elements and then measuring the *activation rate* R, i.e. the number of radioisotopes that each second are created by neutron-induced reactions. The following equation describes the relation between the neutron flux (φ) and the activation rate:

$$R = \mathcal{N} \int \sigma(E)\varphi(E)dE$$

where $\mathcal{N}$ represents the number of precursor isotopes in the irradiated sample and $\sigma(E)$ is the activation cross section. The *effective cross section* (σ_{eff}), i.e. the mean value of the

cross section weighted for the neutron energetic distribution, can be introduced to calculate the integral flux: $\Phi_{TOT} \equiv \int \varphi(E)dE$.

$$\sigma_{eff} = \frac{\int \sigma(E)\varphi(E)dE}{\int \varphi(E)dE} \qquad \Phi_{TOT} = \frac{R}{\mathcal{N}\,\sigma_{eff}}$$

Radioisotopes are mostly produced by neutron capture and they usually decay β^- with simultaneous emission of γ-rays, even if different types of reactions and decays are possible. In any case, if the isotope after the first decay is stable, the differential equation that describes the time evolution of the radioisotope production during the irradiation is:

$$dN = Rdt - N\lambda dt$$

where λ is the decay constant and N the number of radioisotopes in the sample. After the irradiation, the activity of the sample is described by the following law:

$$A(t) = R\left(1 - e^{-\lambda t_{irr}}\right)e^{-\lambda t}$$

where t_{irr} is the irradiation time. Finally, if the measurement of a sample starts after a time t_{wait} and lasts a time t_{meas}, the number of decays that occur is expected to be on average:

$$n_{dec} = \frac{R}{\lambda}\left(1 - e^{-\lambda t_{irr}}\right)e^{-\lambda t_{wait}}\left(1 - e^{-\lambda t_{meas}}\right)$$

Gamma-ray spectroscopy with High Purity Germanium (HPGe) detectors allows to evaluate n_{dec} once the detection efficiency is known for the γ-rays emitted by each radioisotope. A Monte Carlo tool based on the GEANT4 code[1] was developed to simulate the different experimental configurations. Monte Carlo outputs give us the detector simulated energy spectra with a fixed number of decay events (n_{sim}) in the simulated sources. In this way, the efficiency can be evaluated as the ratio between the peaks' counts in the simulated spectra (C_{sim}) and n_{sim} for each γ-ray of interest. Then, the number of decays (n_{dec}) can be calculated for each γ line observed in the experimental spectra through the following relation:

$$n_{dec} = \frac{C_{meas}}{C_{sim}} n_{sim}$$

where C_{meas} are the peaks' counts in the recorded spectra.

2. Irradiations and spectroscopy measurements

Three different irradiation facilities have been used for this experiment: the Central Thimble, the Rabbit Channel and the Thermal Channel. Samples containing many elements with known concentrations were prepared using three Multi-element Calibration Standard solutions by PerkinElmer (Tab. 1).
The standard solutions were put in polyethylene vials filled with blotting paper and their masses were measured using a precision balance (Tab. 2). The samples of Central Thimble and Rabbit Channel were irradiated for 2 hours in November 2011. The irradiation in the Thermal Channel was performed in July 2012 and lasted for 3 hours. In all cases the reactor was working at 250kW power.
The γ-ray spectroscopy of the samples was performed in the days immediately after the irradiations.

Standard Name	Elements	Concentration [µg/mL]
STD 2	Sc, Eu, Lu, La, Sm, Tb, Th, Ho	10.0 ± 1%
STD 3	Ga, U, As, Cd, Cs, Co, Cr, Ag, Se, In	10.0 ± 1%
STD 4	Au, Ir, Sb, Hf, Ru	10.0 ± 1%

Tab. 1: List of the elements in the standard solutions and mass concentration of each element.

Sample	Central Thimble	Rabbit Channel	Thermal Channel
STD 2	0.05169 g	0.05101 g	0.1024 g
STD 3	0.05141 g	0.05076 g	0.1009 g
STD 4	0.05090 g	0.04798 g	0.1010 g

Tab. 2: Masses of the standard solutions used to prepare the samples, the experimental error is the balance sensitivity, i.e. the last decimal place.

Three low background HPGe detectors were employed:

- a coaxial Germanium with a Beryllium window (GePV);
- a coaxial Germanium with an Aluminum end-cap (GeGem);
- a well-type detector with a thin Aluminum end-cap (GePoz).

The GePV detector is installed in a laboratory next to the TRIGA reactor and was used for the short measurements of the irradiated samples just after the extraction from the TRIGA reactor. The GeGem and GePoz detectors are located in the underground Radioactivity Laboratory of Milano-Bicocca University and were used for the medium and long term measurements in a low background environment. In particular, the GePoz is characterized by a high detection efficiency thanks to the well configuration where the irradiated sample are introduced.

Depending on the sample activity, the measurements were performed at different source-detector distances, interposing up to five hollow boxes (1.9 cm high each), in order to have a very low dead time and limit the pile-up counts. The measurements were repeated at different t_{wait} since the irradiation, in order to be sensitive to the elements with lower activity and longer decay time.

3. Activation rate calculation

The activation rate was evaluated for all identified isotopes in the many collected spectra. Each detector-source configuration was modeled with high accuracy and simulations were done for every radioisotope of interest.

The GEANT4 code includes all isotope decay schemes, so that the relative intensities of the many γ-rays emitted and the possible sum peaks generated by the γ cascades are correctly simulated. It's worth noting that this approach was crucial for the analysis of the measurements performed with the samples close to the detector window or inside the well of the GePoz, since in those configurations the probability of sum peaks was at all not negligible. In this way, the activity was accurately estimated even for radioisotopes with complex decay schemes. In order to validate the Monte Carlo tool, various tests were run for every detector and measurement configuration. The detector efficiencies were evaluated at different energies both with specific measurements performed with certified calibrated radioactive multi-gamma sources, and with Monte Carlo simulations describing the measurement configuration. The two efficiencies, evaluated independently, were then compared and they showed a very good agreement, within less than 5%.

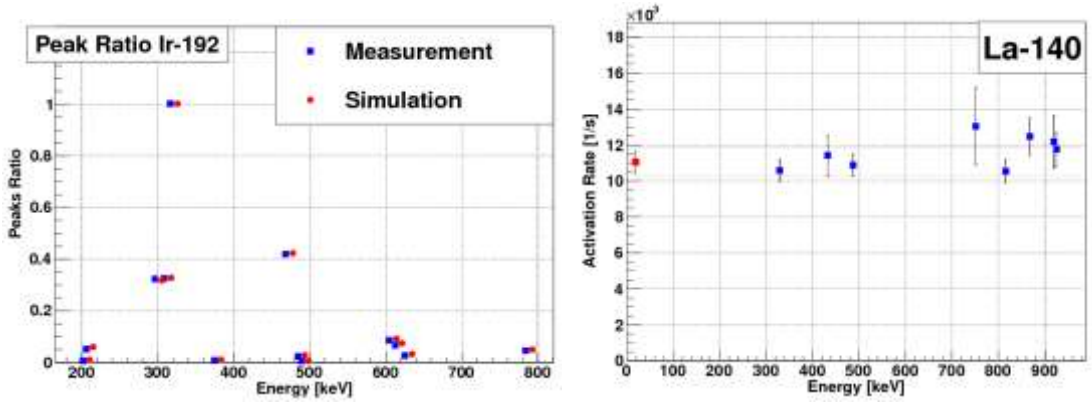

Fig. 1: a) Plot of the ratio between measurement and simulation counts of the peaks of Ir-192 (left). b) Evaluation of the mean value of the La-140 activation rate from the different peaks (right).

When analyzing the experimental spectra, it's possible that different radioisotopes emit γ-rays with the same energy, thus causing peak overlapping. In order to indentify these cases and correctly quantify the peak counts, a graphical tool was developed to visualize the ratios between the intensity of each line in the recorded spectra and in the corresponding simulated ones (Fig. 1a). If a significant discrepancy was observed for a certain γ peak, it was thus possible to investigate the cause and eventually exclude that peak from the analysis. The number of the excluded peaks is anyhow negligible and the overlapping lines have been always identified. The activation rate for a given isotope was finally estimated as the weighted average of the different values obtained from each γ line in its spectrum (Fig. 1b).

The activation rate results from the independent measurements on different detectors were compared and showed a very good agreement. The activation rate per unit mass, which is equal to the *specific saturation activity* (SSA), was evaluated averaging the results obtained from the three different detectors and the standard deviation was used to estimate the associated uncertainty (Tab. 3).

Iso-tope	Central Thimble		Rabbit Channel		Thermal Channel	
	SSA [Bq/g]	Flux [1/s/cm^2]	SSA [Bq/g]	Flux [1/s/cm^2]	SSA [Bq/g]	Flux [1/s/cm^2]
^{46}Sc	(1.99±0.10)10^{12}	(1.67±0.08)10^{13}	(8.70±0.40)10^{11}	(7.19±0.34)10^{12}	(6.86±0.58)10^{10}	(2.69±0.23)10^{11}
^{152m}Eu	(3.33±0.31)10^{13}	(1.70±0.16)10^{13}	(1.43±0.09)10^{13}	(7.19±0.47)10^{12}	(1.02±0.13)10^{12}	(2.47±0.31)10^{11}
^{152}Eu	(6.07±0.85)10^{13}	(1.74±0.24)10^{13}	(2.98±0.79)10^{13}	(8.42±2.23)10^{12}	(2.03±0.21)10^{12}	(2.74±0.29)10^{11}
^{177}Lu	(2.34±0.22)10^{12}	(1.87±0.18)10^{13}	(8.96±0.65)10^{11}	(7.13±0.52)10^{12}	(6.46±0.63)10^{10}	(2.72±0.27)10^{11}
^{140}La	(2.30±0.05)10^{11}	(1.70±0.04)10^{13}	(1.04±0.04)10^{11}	(7.50±0.27)10^{12}	(7.52±0.54)10^{9}	(2.70±0.20)10^{11}
^{153}Sm	(2.37±0.10)10^{12}	(1.70±0.08)10^{13}	(1.00±0.05)10^{12}	(6.96±0.33)10^{12}	(4.63±0.40)10^{10}	(2.42±0.21)10^{11}
^{160}Tb	(1.14±0.14)10^{12}	(1.82±0.23)10^{13}	(4.61±0.36)10^{11}	(7.05±0.56)10^{12}	(1.95±0.16)10^{10}	(2.40±0.20)10^{11}
^{233}Pa	(2.13±0.15)10^{11}	(1.96±0.14)10^{13}	(8.52±0.56)10^{10}	(7.45±0.50)10^{12}	(4.76±0.94)10^{9}	(2.99±0.59)10^{11}
^{154}Eu	(5.27±1.51)10^{12}	(1.80±0.51)10^{13}	(1.72±0.20)10^{12}	(5.71±0.67)10^{12}	(1.40±0.41)10^{11}	(2.58±0.75)10^{11}
^{166}Ho	(2.23±0.10)10^{12}	(1.70±0.08)10^{13}	(9.80±0.68)10^{11}	(7.28±0.51)10^{12}	(5.12±0.81)10^{10}	(2.60±0.41)10^{11}
^{72}Ga	(1.26±0.05)10^{11}	(1.61±0.07)10^{13}	(5.58±0.26)10^{10}	(6.89±0.33)10^{12}	(3.16±0.32)10^{9}	(2.46±0.25)10^{11}
^{239}Np	(2.56±0.24)10^{11}	(1.51±0.15)10^{13}	(1.12±0.07)10^{11}	(6.28±0.42)10^{12}	(2.47±0.23)10^{9}	(1.94±0.19)10^{11}
^{76}As	(3.58±0.18)10^{11}	(1.55±0.08)10^{13}	(1.54±0.10)10^{11}	(6.39±0.41)10^{12}	(6.73±0.90)10^{9}	(2.13±0.28)10^{11}
^{115}Cd	(1.01±0.10)10^{10}	(1.61±0.16)10^{13}	(4.67±0.50)10^{9}	(6.93±0.75)10^{12}	(1.23±0.19)10^{8}	(2.21±0.35)10^{11}
^{134}Cs	(1.42±0.04)10^{12}	(1.70±0.06)10^{13}	(6.16±0.19)10^{11}	(7.06±0.24)10^{12}	(2.87±0.29)10^{10}	(2.45±0.25)10^{11}
^{60}Co	(2.49±0.24)10^{12}	(1.80±0.17)10^{13}	(1.09±0.12)10^{12}	(7.71±0.84)10^{12}	(7.39±0.73)10^{10}	(2.71±0.27)10^{11}
^{51}Cr	(4.67±0.42)10^{10}	(1.83±0.17)10^{13}	(2.24±0.17)10^{10}	(8.69±0.68)10^{12}	(1.63±0.26)10^{9}	(3.00±0.49)10^{11}
^{110m}Ag	(1.24±0.07)10^{11}	(1.51±0.09)10^{13}	(5.17±0.29)10^{10}	(6.00±0.34)10^{12}	(2.32±0.17)10^{9}	(2.03±0.15)10^{11}
^{75}Se	(3.42±0.18)10^{10}	(1.74±0.09)10^{13}	(1.49±0.16)10^{10}	(7.39±0.81)10^{12}	(8.06±1.71)10^{8}	(2.74±0.58)10^{11}
^{114m}In	(2.65±0.24)10^{10}	(1.84±0.17)10^{13}	(1.19±0.12)10^{10}	(7.89±0.77)10^{12}		
^{198}Au	(3.40±0.10)10^{12}	(1.67±0.06)10^{13}	(1.61±0.11)10^{12}	(7.45±0.53)10^{12}	(6.57±0.48)10^{10}	(2.34±0.18)10^{11}
^{192}Ir	(7.06±0.28)10^{12}	(1.57±0.07)10^{13}	(3.51±0.23)10^{12}	(7.68±0.51)10^{12}	(2.18±0.16)10^{11}	(2.63±0.20)10^{11}
^{194}Ir	(2.22±0.07)10^{12}	(1.71±0.06)10^{13}	(1.05±0.05)10^{12}	(7.71±0.38)10^{12}	(4.80±0.30)10^{10}	(2.50±0.16)10^{11}
^{122}Sb	(3.10±0.11)10^{11}	(1.65±0.06)10^{13}	(1.45±0.09)10^{11}	(7.35±0.47)10^{12}	(4.24±0.31)10^{9}	(2.20±0.16)10^{11}
^{124}Sb	(1.37±0.04)10^{11}	(1.67±0.06)10^{13}	(6.52±0.48)10^{10}	(7.33±0.55)10^{12}	(1.87±0.19)10^{9}	(2.08±0.21)10^{11}
^{181}Hf	(1.06±0.12)10^{11}	(1.86±0.21)10^{13}	(5.69±0.90)10^{10}	(9.77±1.55)10^{12}	(3.74±1.32)10^{9}	(3.34±1.18)10^{11}
^{103}Ru	(1.43±0.02)10^{10}	(1.42±0.03)10^{13}	(7.95±0.76)10^{9}	(7.71±0.75)10^{12}	(4.35±0.41)10^{8}	(2.45±0.23)10^{11}

Tab. 3: Specific saturation activity and flux results from the different activated radioisotopes.

4. Flux results

The effective cross section depends on the neutron spectrum distribution, that is different in each irradiation facility. For this purpose, the MCNP[2] model of the Pavia TRIGA reactor, developed and benchmarked in the recent years[3], is exploited to evaluate the neutron energetic distributions. The integral contained in the σ_{eff} definition was numerically calculated by subdividing the energy axis in 135 bins and by using the ENDF[4] pointwise cross section data.
The neutron flux results are shown in Tab. 3 for all the radioisotopes that were analyzed. The good agreement among the results from the different isotopes shows that the neutron energetic distributions estimated by means of MCNP simulations are correct and allow a precise evaluation of the effective cross sections.

The flux mean value was calculated for each irradiation facility (see Tab. 4) and the standard deviation was calculated to estimate the uncertainty and the degree of compatibility among the results. Finally, a benchmark analysis of the MCNP simulation model was performed by comparing the measured flux values with the ones calculated through the MCNP simulations (Tab. 4). The good agreement observed for the Central Thimble and the Rabbit Channel, points out that reactor core is well described in the simulations. On the contrary, the model should be improved in the reflector region, because a significant discrepancy is recorded for the Thermal Channel. For this reason, we are planning to include a more realistic description of the reflector materials in the simulation model, keeping into account the non-ideality of the graphite.

	Meas. Flux [1/s/cm^2]	MCNP Flux [1/s/cm^2]
Central Thimble	(1.70 ± 0.13) 10^{13}	(1.88 ± 0.02) 10^{13}
Rabbit Channel	(7.34 ± 0.81) 10^{12}	(8.39 ± 0.17) 10^{12}
Thermal Channel	(2.52 ± 0.32) 10^{11}	(5.83 ± 0.09) 10^{11}

Tab. 4: Measured and simulated neutron flux results in the TRIGA irradiation facilities.

5. Conclusions

An absolute measurement of the neutron flux was performed by means of the NAA technique in three irradiation facilities of the TRIGA Mark II reactor of the University of Pavia. The γ-ray spectroscopy measurements were analyzed with the help of GEANT4 Monte Carlo simulations, that were crucial for a very precise evaluation of the detection efficiency. The good agreement between the measurements on different HPGe detectors confirms the reliability of this methodological approach. The neutron flux was calculated using the data of radioisotopes activated with different cross sections, obtaining a very good agreement in the results. In such a way, the integral flux was finally evaluated with a precision around 7% for Central Thimble and 12% for Rabbit and Thermal channels.

References

1. https://geant4.web.cern.ch/geant4/ and the "Physycs Reference Manual" therein.
2. Monte Carlo Team. *MCNP - A general Monte Carlo N-Particle Transport Code, Version 5*. LA-UR-03-1987. Los Alamos National Laboratory, April 24, 2003.
3. A. Borio di Tigliole, A. Cammi, M. Clemenza, V. Memoli, L. Pattavina and E. Previtali. *Benchmark evaluation of reactor critical parameters and neutron fluxes distributions at zero power for the TRIGA Mark II reactor of the University of Pavia using the Monte Carlo code MCNP.* Progress in Nuclear Energy, 2009.
4. http://www.nndc.bnl.gov/exfor/endf00.jsp and the "ENDF/B-VII.1 Nuclear Data for Science and Technology" document therein.

EXPERIMENTAL INSTRUMENTATION FOR MEASUREMENT OF REACTIVITY TEMPERATURE AND VOIDING EFFECTS AT ZERO POWER RESEARCH REACTORS

T. BILY, L. SKLENKA
Department of Nuclear Reactors, Czech Technical University in Prague
V Holesovickach 2, 18000 Prague 8 – Czech Republic

ABSTRACT

Temperature and void reactivity effects play an important role in ensuring safe operation of nuclear reactors. To better understand and examine the effects, an experimental instrumentation has been developed at VR-1 reactor of Czech Technical University in Prague. The instrumentation utilizes the obvious advantages of zero power reactors – physically fresh and well-defined core enabling precise modelling and analysis; and negligible amount of heat produced by chain reaction. Thus, a temperature change or voiding effect can be induced in a controlled way in well-defined part of the core by an external mean and reactor response to such change can be examined and understood. The loop-type tailor-made instrumentation is capable to cause temperature increase in fuel assemblies and surrounding moderator (i.e. isothermal reactivity effects can be induced) or voiding in the area corresponding to 2x2 positions of reactor grid (ca. 14 x 14 cm). Standardly, four 8-tube fuel assemblies of IRT-4M type are used as an experimental module; however, due to modular design of the loop, in principal, any type of experimental module can be used. The instrumentation is based on external water-heater and pressurized-air based bubble-makers and enables inducing both reactivity effects separately or coupled. Beside thermometers, the loop is further equipped with pressure, and flow rate sensors; thus, the experimental data could be further used for various benchmarking purposes. Being installed at university reactor, the instrumentation could be utilized for educational and training purposes as well. The paper describes the instrumentation, its operational parameters, fields and ways of its utilization as well as issues connected to its implementation into the reactor core.

1. Introduction

Recently, a new experimental instrumentation for demonstrating and studying temperature and voiding reactivity effects was designed [1,2,3] and installed in the VR-1 reactor. This instrumentation further extends experimental as well as educational capabilities of the reactor that have been gradually developing since the reactor was put in operation in 1990.

2. VR-1 Reactor

VR-1 is a light-water zero power pool-type training reactor operated by the Czech Technical University in Prague. The core consists of tubular IRT-4M tube assemblies (enrichment on 19.7% of 235-U, see fig. 1). As the reactor is mainly utilized for education and training purposes, the reactor is heavily equipped with experimental equipment that enable to study various core physics phenomena (e.g. delayed neutrons, reactor kinetics, voiding effects).

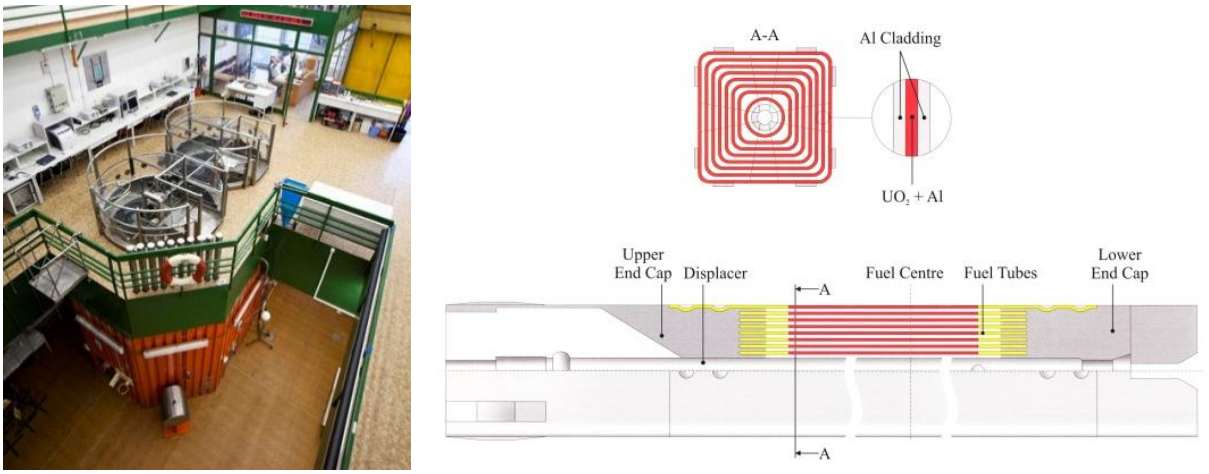

Fig. 1: Left:VR-1 reactor; Right: IRT-4M fuel assembly

3. Instrumentation

3.1. Principle of Operation

The instrumentation has a form of hot water loop (see fig. 2) which enables heating of an experimental module placed inside the reactor core up to the temperature of 70°C. In current setup, the IRT-4M fuel assemblies are used as experimental module. Thus, according to the fuel operational limits and conditions only the operation below 45°C is allowed. Water heated in external heater is led to experimental module in the core through the bottom tube sheet which is firmly connected with the core support grid (see fig. 3); then it flows through the module, heats it up, and follows through the upper tube sheet to volume compensator, and pump back to the heater. Thus an area inside the core with elevated temperature is established and its reactivity temperature effects could be measured.

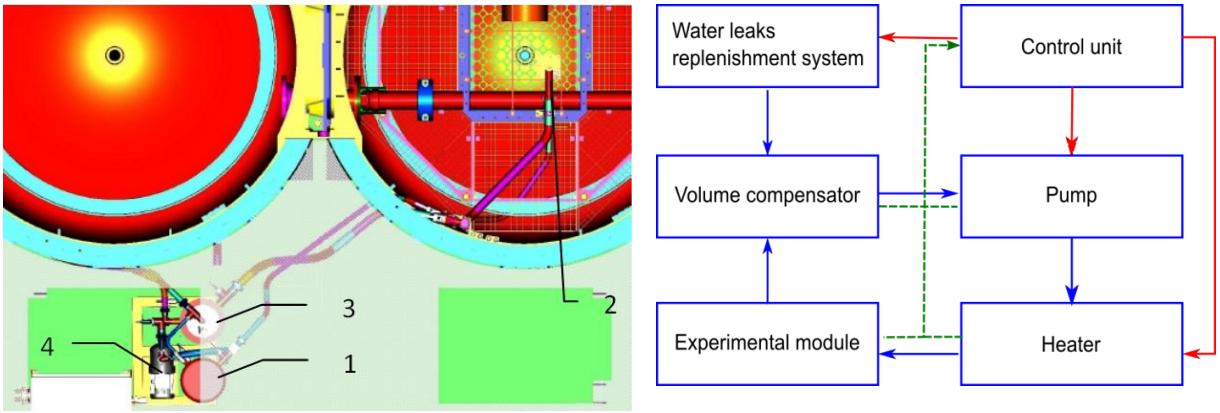

Fig. 2: Instrumentation for temperature reactivity effects demonstration and measurement at VR-1 reactor. Left: 1-heater,2-module in the core, 3- volume compensator, 4- pump.Right: Functional scheme: blue line – water loop; green line – data acquisition; red line – control. [1]

Voiding feature is achieved by pressurized air led to bottom tube sheet of the experimental module (see fig. 3). From the bottom tube sheet the air is led through bubble-makers which are situated at the top part of reactor grid below fuel assemblies. The pressurized air passage through the core support grid is accomplished by hollow screws, four of which are used for fixing the bottom tube sheet to core support grid as well. In this way up to 20 hollow screws with bubble makers attached to their upper endings can be used to provide uniform bubble generation within the experimental module. The generated bubbles then flow into the module in the core, pass it through and are separated from the water at volume-compensator

vessel. The amount of generated bubbles (the pressurized air flow) is controlled through the control unit of device for bubble boiling study [4] placed close to the loop control unit.

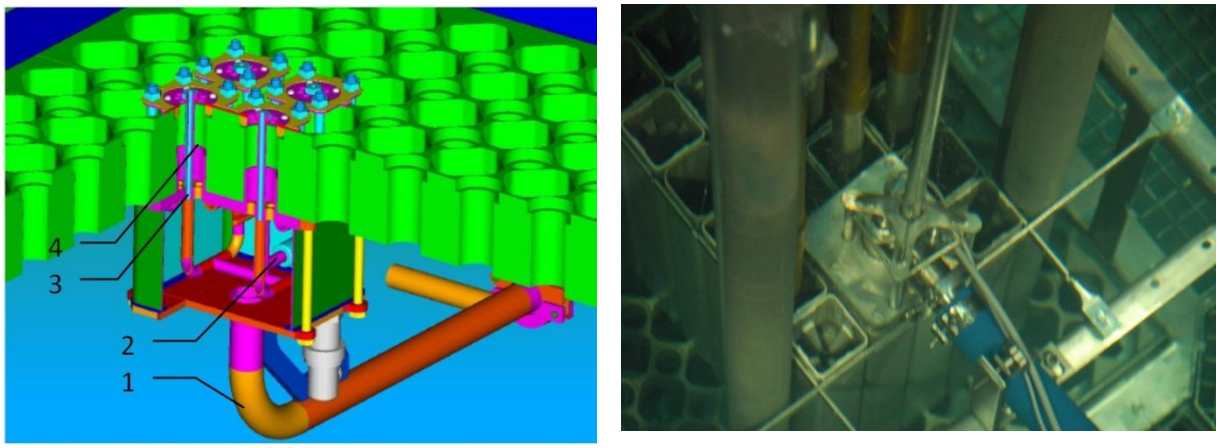

Fig. 3: Left: Bottom tube sheet. 1- water inlet, 2- pressurized air inlet, 3 – pressurized air passage tube; 4 – water passage channel [1] Right: Upper tube sheet

3.2. Instrumentation Control

The loop operation is controlled through the control unit with a touchscreen enabling setting the required parameters and observing the operational data (see fig. 4). The unit enables control of the heater through desired core inlet temperature. This temperature could be reached either by given constant heating power (0-20kW) or by utilizing full heater capacity and autotunig PID control algorithm.

Fig. 4 Touch-screen of the instrumentation control unit

In case of two phase operation the amount of water and bubbles in the loop have to be controlled. This task is achieved by automatic water replenishment system based on water level measurement in volume compensator vessel and by setting its required and minimal value; in case the stated minimal limit is reached, the water is fed to the volume compensator from standard circulating system of the VR-1 reactor using two electrically controlled valves that can switch temporarily the flow of standard circulating system towards the loop. The first valve situated on the leg leading water to the core (in base mode being opened) is closed and the second one on the leg leading water to the loop volume compensator (in base mode closed) gets open; thus the water is being refilled till the required water level is reached. Meanwhile, the corresponding amount of air is removed.

To understand the loop behaviour, it is further equipped with several temperature, pressure and flow rate sensors enabling measurement of such parameters at various parts of the loop during operation. Based on some of these measurements, instrumentation protection is implemented (pump protection, overheating protection).

3.3. Experimental module

Under the term “experimental module” the heated part of reactor core covering 2x2 positions of reactor grid is mentioned. The module can be placed at any grid position with the exception of positions around neutron source injection system (core centre). Currently, four eight-tube IRT-4M fuel assemblies with inner displacers are used as experimental module. Of course, in such arrangement, neither thermal, nor water-tight isolation could not be fully achieved. Some heat transfer takes place through fuel assembly outer surfaces; leaks/influxes can occur in the point of the fuel assemblies’ conjunction with their bottom and upper tube sheets. However, during the functional tests of the instrumentation, this heat transfer was pretty small leading to the temperature increase in the module surroundings below 1°C at loop operating at 40°C. Thus, this module is convenient especially for educational purposes and for demonstration of particular reactivity effects because it utilizes the same fuel type as is used in the rest of the core. For high precision temperature effects measurements, another module would be needed.

3.4. Loop materials

One of the main tasks of the instrumentation is to heat up the experimental module in the core while remaining other parts at unchanged temperature. Of course, as currently IRT-4M fuel assemblies are used as experimental module, there will still be some heat transfer to the rest part of the core. However, where possible, the materials with low thermal conductivity were chosen, especially for piping and tubing (TECAMID 6, CALORTEC 165LE). Minor parts of the loop were constructed from austenitic steel as well (bottom and top tube sheets of the experimental module, valves …).

4. Implementation

The instrumentation for temperature and void effects measurements would became an inherent part of the VR-1 reactor core. Therefore, a new core configuration called C8 (see fig. 5) has been designed and implemented. The core configuration enables reaching adequate reactivity changes by the instrumentation as well as the proper operation of other experimental instrumentations and devices routinely used at VR-1 reactor (devices for delayed neutron studies, dynamic effects studies, void effect studies, etc).

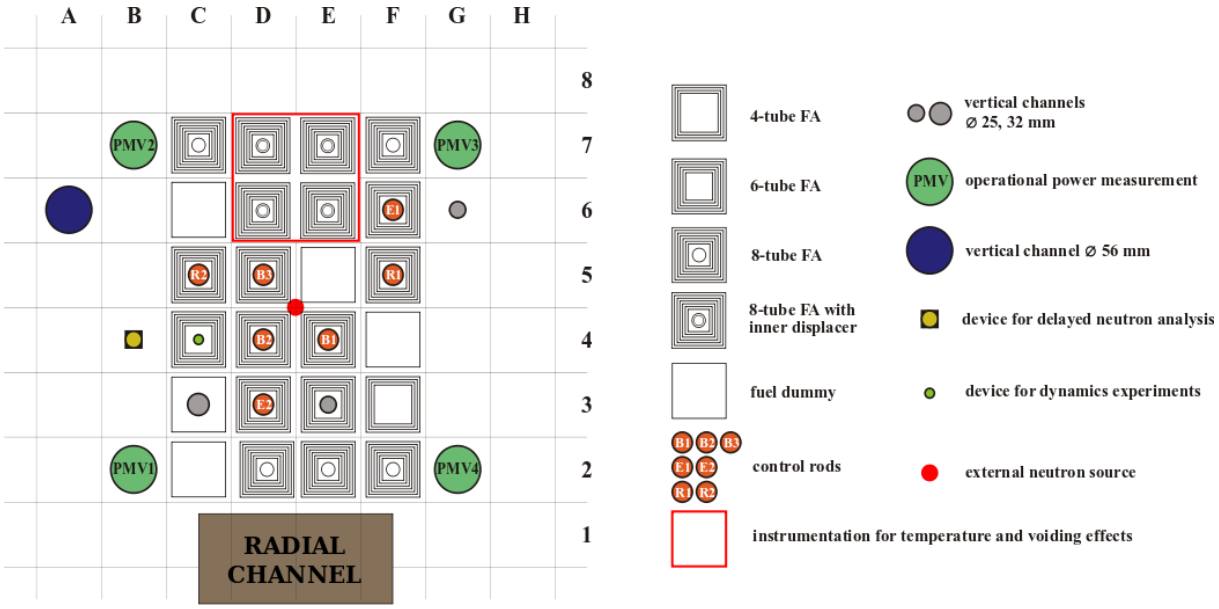

Fig. 5 Core configuration C8 with implementation of instrumentation for temperature and void effects

5. Operational parameters

The basic parameters of the loop are temperature ranges, water and bubble flow rates, heating power. Power of the heater could be set within 0 to 20 kW. The water flow rate could be controlled by circulation pump parameters. The pump can be operated from 1000 rpm (which corresponds to ca. 15 l/min) to 2900 rpm (ca. 50 l/min). The bubble flow rate can be changed by device for voids effects study. So far, loop stability has been proved till 350 ml/min The temperature in the experimental module could be changed from ambient one (ca. 20°C) to 45°C (being operational limits and conditions limit for fuel water-inlet-temperature).The temperature is measured at the core inlet, core outlet, volume compensator inlet and heater outlet. The core inlet temperature is further used for heater control.

6. Fields of utilisation

In current setup, the instrumentation is devoted mainly for demonstration of individual reactivity effects aiming on educational and training activities. The instrumentation can be operated in two modes. It enables either to cause temperature changes by the heater, or void changes by bubble makers. Thus, the isothermal temperature reactivity coefficient and void coefficient of reactivity of the experimental module can be measured for several temperatures between the ambient one up to the desired maximal one, or different bubble flow rates respectively.

Furthermore, both effects can be studied together. Finally, the water replenishment system can be further used for simulation of cold water injection into the hot loop. Generally, the generated reactivity changes are rather small, but well measureable. They reach some 0.1$ which corresponds to rod movement of ca. 30 mm in case of heating from 23°C to 38°C; the bubble effect causes rod movement of another 13 mm for air flow rate change from 0 to 350 ml/min.

Temperature reactivity effects represent the base mode of the instrumentation operation. In this mode of operation, the isothermal temperature coefficient of the experimental module could be measured for several temperatures between the ambient one up to the desired maximal one. It should be noticed that the structure of temperature reactivity changes will depend on selected experimental module and on position of the module in the core (i.e. on its surroundings).

The measurement on the loop can be performed either with subcritical reactor with external neutron source by subcritical multiplication theory or at critical state of the reactor controlled by automatic system (by monitoring rod movement). Examples of operation from first tests of the instrumentation are shown in fig. 6 and 7 (loop cooling down from ca. 40 to 20 °C, nad void effect respectively). Figure 6 shows a screenshot from operator's screen. The reactor was operated in automatic mode of operation. In this mode, the automatic regulator operates the reactor at a set constant power (red line in the figure); any reactivity changes are compensated by automatic rod movement. The temperature of the loop was ca. 40°C. Then, the loop heating was switched off, and utilizing water replenishment system, the temperature in the loop was gradually decreased to some 20°C. Decrease in water temperature in under-moderated area, as well as decrease of fuel temperature in experimental module cause positive reactivity effect which is compensated by control rod insertion (rod position is indicated by violet line). The blue line indicates power rate in % of power change per second. It could be seen that the whole process run smoothly without any fast power changes. Figure 7 illustrates void effect in experimental module. Reactor was operated in subcritical mode (ca. -0.5 $) with external neutron source and subcritical multiplication count rate was measured. Gradually, in the experimental module the level of bubble flow rate was increasing (in steps from 100 to 350 ml/min). The higher amount of bubbles, the higher is the voiding in the experimental module. As the module is under-moderated, the negative reactivity effect is induced. Thus, gradual decrease of subcritical multiplication count rate can be observed (blue line).

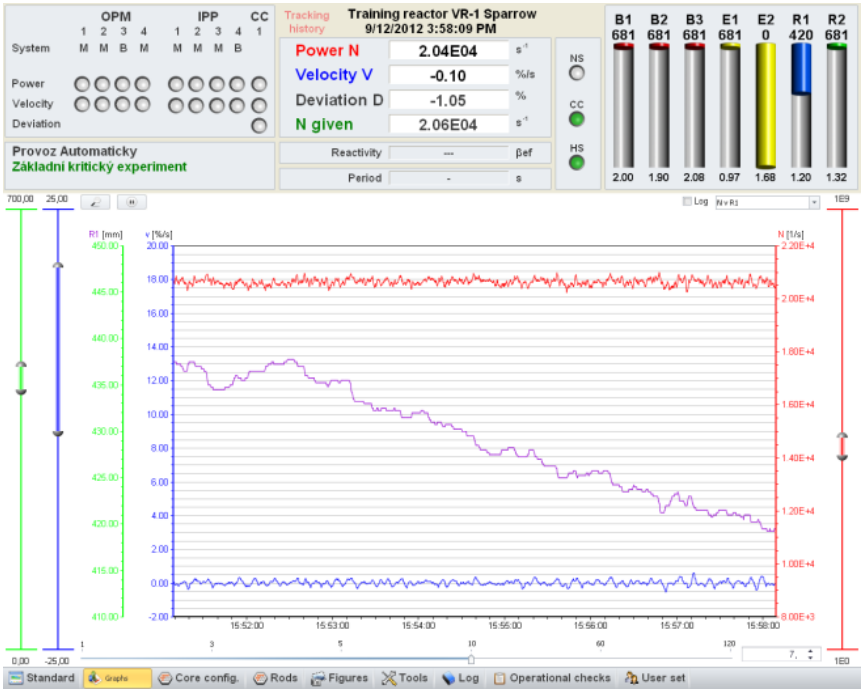

Fig. 6: Demonstration of temperature reactivity effect in critical reactor

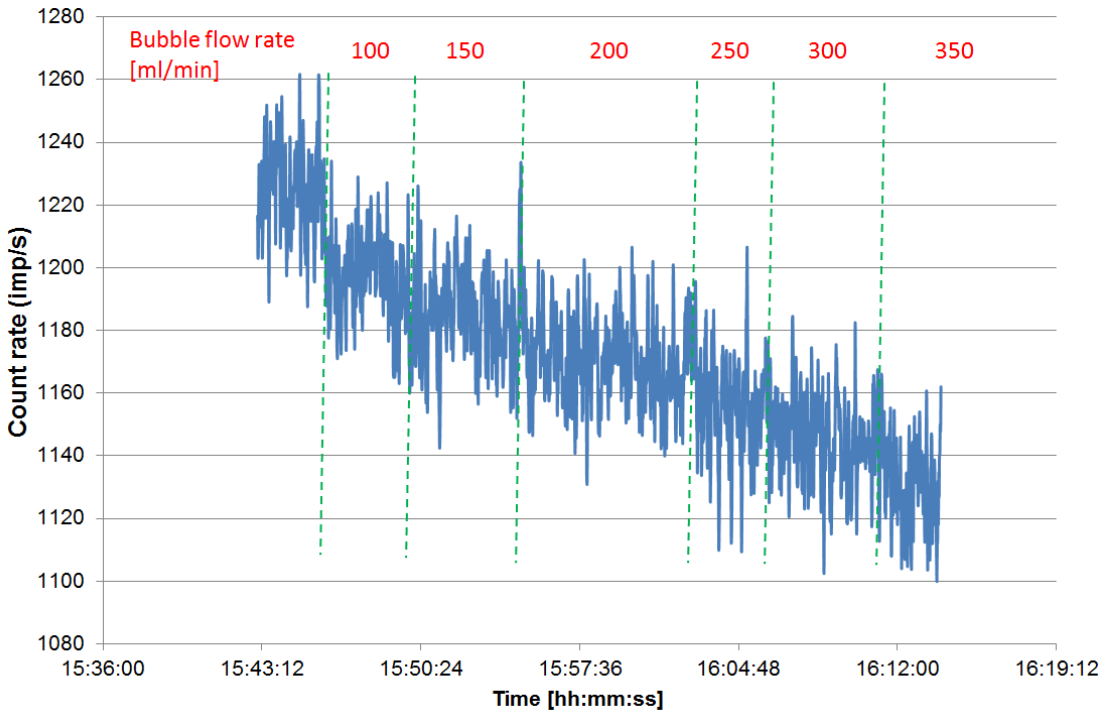

Fig. 7: Demonstration of reactivity void effect in subcritical reactor

7. Further work

The further activities are connected mainly with two issues: loop control and data acquisition, and on experimental module.

First, an option to control the loop via a standard computer is supposed. This would further extend the loop experimental capabilities as more complex sequences would be programmed in a form of batch file. Also, the loop operational data could be in this case directly connected within the operational data of the reactor control system through a software “Experimental Studio” [5], already in use at the reactor to analyse the operational

data. Thus, more complex processes would be simulated by the instrumentation and analysed easily together with reactor response.
Second, another experimental module is thought, that would enable higher precision temperature reactivity effects measurements. It is supposed to be assembled from EK-10 pins that are available at the department. Due to pins geometry the module could be designed as thermally isolated from the core without any leaks, moreover, with the possibility of reaching higher temperatures (up to 70°C).

8. Conclusions

At VR-1 reactor, a new instrumentation for temperature and void effects induction and measurement was developed and implemented in the reactor core. The first tests confirmed the design expectations were met. Thus, the instrumentation has a big potential to become valuable educational as well as experimental tool.

References:

[1] Beneš, V., Zahradil, L., Němec, P.: Experimental educational instrumetation for studiing the temperature reactivity effect: Technical description, ŠKODA-JS a.s., 2011 (available in Czech only)

[2] Bily T., Sklenka L.: Neutronic Design of Instrumentation for Thermal Effects Measurement on VR-1 Reactor, ANIMMA International Conference, 7-10 June 2009, Marseille, France

[3] Bily T., Sklenka L.: Study of Temperature Reactivity Effects on Zero Power Reactor for Increasing Safe Operation of Nuclear Installations Electric Power Engineering 2012

[4] Sklenka, Ľ., Rataj, J., Teplý J., Nádeník T: BUBLINKY - instrumentation for simulation of bubbly boiling - void coefficient studies, Technical report, 2008

[5] Rataj, J. - Reisner, L. - Sklenka, L.: Experimental Studio – New Data Acquisition System for Extended Education and Training at VR-1 Reactor. IAEA Conference on Research Reactors: Safe Management and Effective Utilization, Rabat, Morocco 2011

DESIGN AND SIMULATION OF THE SAFETY SYSTEMS FOR A NUCLEAR TEST FACILITY WITH SUPERCRITICAL WATER

M. Raqué
EnBW Kernkraft GmbH
Rheinschanzinsel, 76661 Philippsburg - Germany

T. Schulenberg
Karlsruhe Institute of Technology
Hermann-von-Helmholtz-Platz 1, 76344 Eggenstein-Leopoldshafen – Germany

ABSTRACT

In a European project, called SCWR-FQT (Fuel Qualification Test) an in-pile fuel assembly test is planned in the Czech research centre CVR in Řež in order to examine material and thermal-hydraulic behaviour of the fuel under supercritical pressure. The test section will be operated at temperatures and pressures, which are typical for the European High Performance Light Water Reactor (HPLWR) concept [1]. The test fuel element, composed by a pressure tube containing 4 UO_2 fuel rods, is connected to a closed 300 °C loop with the test section handling infrastructure. In order to assure a safe operation, the loop is equipped with diverse independent safety systems.
This paper describes a one-dimensional model, which was set up using the system code APROS in order to evaluate and optimize the performance of the safety systems. For several loop components the modelling is presented in detail. Furthermore, the simulation results for an automatic depressurization transient prove that the safety systems and long-term residual heat removal strategy are functioning as desired.

1. Introduction

In the framework of the supercritical water cooled reactor (SCWR) development, an in-pile fuel assembly test is planned in the Czech research centre CVR in Řež in order to examine material and thermal-hydraulic behaviour of fuel rods under supercritical pressure. In this European project, called SCWR-FQT (Fuel Qualification Test), a supercritical water cooled reactor test fuel element is intended to be inserted into the existing pool type research reactor LVR-15. The test section will be operated at temperatures and pressures, which are typical for SCWR conditions. A thick-walled pressure tube made out of austenitic steel, able to withstand the high system pressure, encloses the test section. It contains four fuel rods with a total heating power of 63.6 kW and a recuperator in order to achieve hot channel conditions. Furthermore, a U-tube cooler in the head of the fuel element serves as heat sink. An air gap between pressure tube and the reactor pool insulates the test fuel element. The test section is connected via a 300 °C closed loop to a recirculation pump and the test section handling infrastructure, which is located outside the reactor building. Furthermore, a combination of active and passive safety systems, described by Raqué et al. [2], ensure a safe operation of the loop.

In order to evaluate the performance of these safety systems under various postulated accident scenarios, a one-dimensional model of the loop was set up using the commercial system code APROS. The model can simulate fast transients including depressurization to sub-critical conditions, as they may occur e.g. during loss of coolant accidents. Details of the numerical model and simulation results for a depressurization transient are presented exemplarily.

2. System code APROS

For optimization of safety system design parameters, a one-dimensional model of the loop with all safety relevant components has been set up. The numerical code used for this task is the commercial system code APROS (Advanced Process Simulation) [3] developed by VVT Finland and Fortum. The code is already widely-used in the field of nuclear and combustion power plants. Apart from its common use, the code shall be applied here for modelling a nuclear facility with supercritical water. For this reason, APROS version 5.09 was used as it features an extension of the thermodynamic properties for water and steam to the supercritical pressure region in accordance to the international standard IAPWS-IF97. Furthermore, Kurki [4] implemented pressure loss and heat transfer correlations for supercritical water. The code modifications enable the simulation of depressurization transients from supercritical to subcritical pressures.

Choosing a six equation two-fluid model for supercritical and for subcritical conditions allows a reliable and accurate computation of the process state using a detailed physical description. The model of Hänninen et al. [5] is based on the one-dimensional conservation equations of mass, momentum and energy, which are applied to the liquid and the gas phase. Kurki [4] extended the model to supercritical pressures. From this system of six partial differential equations, the pressures, void fractions, phase velocities and phase enthalpies are solved. Furthermore, the two phases are coupled by empirical friction and heat transfer correlations.

3. Emergency systems

The loop is equipped with diverse independent safety systems, schematically depicted in Figure 1, to ensure safe operation. In case of emergency, the loop is depressurized over the automatic depressurization system, which contains three depressurization lines and a pressure suppression tank (BN). Moreover, two separate emergency coolant injection systems are preventing damage of the fuel rods due to over temperatures. Each of them consists of an emergency cooling injection pump in combination with a 30 litre pressure accumulator (TZ). The passive bladder accumulators will provide their inventory as soon as the system pressure drops and thus give a grace period for the according pump to start up. Both systems are fed by a reservoir (HN1) containing 1.7 m^3 of water.

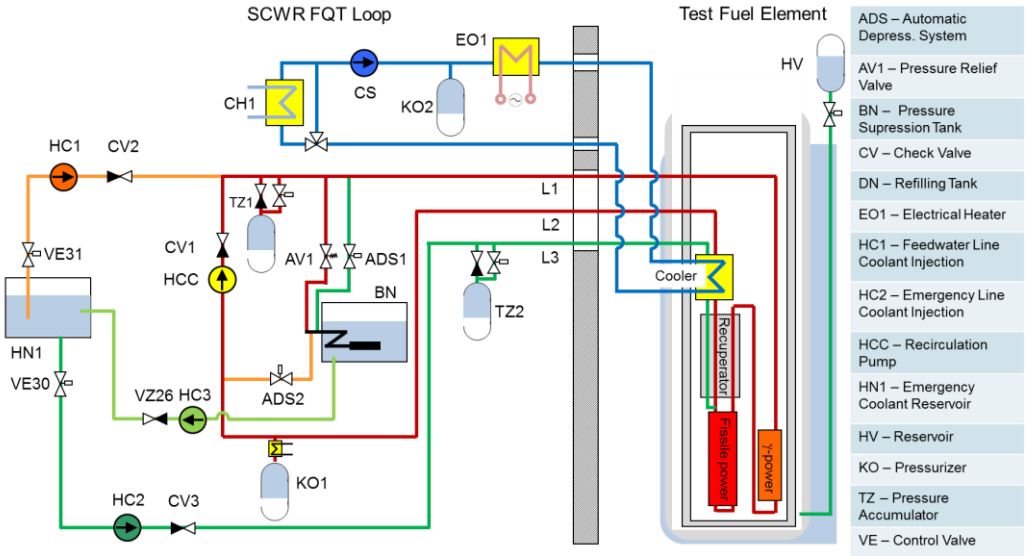

Fig 1. Schematic illustration of the SCWR-FQT loop.

The first safety system called FLCI (Feed water Line Coolant Injection, orange) system injects coolant into the feed water line (L1), e.g. in case of a trip of the recirculation pump (HCC). The ELCI (Emergency Line Coolant Injection, dark green) system instead, which serves as a backup for the FLCI system, injects coolant directly on top of the fuel rods over

an additional emergency coolant line (L3), exclusively used in case of a loss of coolant accident. A connecting line between the depressurization tank and the reservoir (light green) enables a closed coolant circulation for long-term residual heat removal. During normal operation at a pressure of 25 MPa, another bladder accumulator is utilized as pressurizer (KO1). A U-tube cooler in the top of the test fuel element forms the heat sink of the system. The connected secondary circuit (blue) is also operated at a pressure of 25 MPa. In case of an accident, the reactor pool can serve as a secondary heat sink by filling an isolation gap between fuel element and reactor pool with water. Thus, the heat transfer over the pressure tube is enhanced, keeping the material temperature within the limit of 400 °C.

4. Component modelling

4.1 Heated section

The heated section is located in the bottom part of the test fuel element. It consists of four UO_2 fuel rods of 60 mm length with a fissile power of 15.9 kW each. Together with a gamma power of 9.8 kW, the total heating power equals to 73.4 kW. The heated section is enclosed by the assembly box, which forms the central of four concentric flow channels. These four channels are consecutively passed through by the coolant from outermost to innermost. With such a flow path, high coolant temperatures at the fuel rods of around 480 °C can be realized, simultaneously meeting the material limit of the pressure tube. Figure 2 shows the modelling of the heated section with APROS.

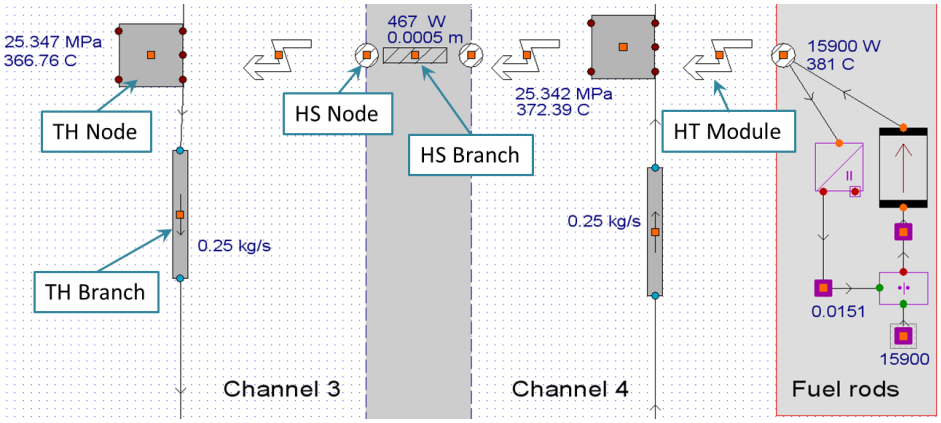

Fig 2. One segment of the heated section modelled with APROS.

In axial direction, the heated section is discretised by four segments of equal length. The flow channels are modelled by the use of a node (TH Node) and a branch (TH Branch) for each segment. In the staggered grid discretization of APROS, the variables of state, pressure and enthalpy are computed in the centre of a node resembling a computational cell. These nodes describe the shape of the flow volume. A branch resembles the border of a computational cell and links to nodes. Here, mass flow and pressure loss are evaluated.
To model the heat transfer over the wall between two nodes, located at the same height of two neighbouring channels, three different component types are used, as depicted in Figure 2. The two surfaces of a wall are modelled by two heat structure nodes (HS Node). These nodes are described by the coordinate system, their heat transfer area and their angle towards the horizontal to compare it to the flow direction. Here, the surface temperature is calculated. Two heat structure nodes are connected by a heat structure branch (HS Branch). By choosing the appropriate wall material and thickness the heat flow over the wall can be evaluated. A heat transfer module (HT Module) connects a heat structure branch with a thermal hydraulic node of the flow volume. To calculate the heat transfer coefficient, the heat transfer area as well as the thermal hydraulic diameter must be entered.
The heat input of the fuel rods is modelled similar to the heat transfer over a wall. For this reason, the fissile power is equally subdivided to the four segments of the heated section. The heat flux to the respective thermal hydraulic node is evaluated via a boundary condition

module and the heat transfer area of a heat structure node. By setting the variable number of parallel heat structures to 4, all fuel rods can be modelled collectively.
The heat input, generated in the metal structures of the fuel element by gamma irradiation is modelled similarly. Here, the total power of 9.8 kW is subdivided to the five walls composing the four sub-channels, in relation to their mass fraction. Thus, 90 % of heat is released in the thick-walled pressure tube.
The modelling of the recuperator and cooler sections is done accordingly.

4.2 Depressurization system

The depressurization of the primary circuit is carried out via three depressurization lines, one opened by a spring loaded pressure relief valve (AV1), which is automatically activated in case the system pressure exceeds 26 MPa, and one for each of the two emergency systems (ADS1, ADS2). Behind the valves, the three lines come together in a single line, ending up submerged in the water storage of the depressurization tank. The open end of the depressurization line is designed as a sparger, consisting of 50 holes of 2 mm diameter arranged in ten rows with a pitch of 10 mm. The vented depressurization tank works as the pressure sink of the loop. Furthermore, bubbles or steam jets shall be condensed without penetrating the water surface. The gas volume of the tank must be capable to take over the coolant injected by the pressurizer and the accumulators. Nitrogen is considered for venting since hydrogen from radiolysis could be accumulated here. A water volume of 0.63 m^3 is big enough to keep the coolant temperature below saturation temperature for any kind of accident. For a tank of 1 m in diameter and a height of 1.5 m this adds up to a liquid level of 0.8 m during normal operation of the loop.
For the numerical system analysis, the porous end of the sparger tube is modelled by a node with respective volume. The 50 sparger holes are resembled by a single pipe module, whose flow length of 4 mm corresponds to the wall thickness of the depressurization line. For the evaluation of the pressure drop the hydraulic diameter for one hole of 2 mm is used in combination with the total flow area of all holes. A discharge coefficient of 1 is applied.
Flow through the holes is limited to the critical mass flow when the maximum speed at the narrowest cross section reaches sound velocity. For liquid single-phase and for two-phase flow the critical flow is calculated according to Moody [6]. In case the two-phase flow is changing to steam flow, a linear interpolation between the Moody model and a single-phase Laval nozzle is applied.
The pipe is connected to a tank module, which is defined by its geometry and the variables pressure, temperature, enthalpy, liquid level, and the mass fraction of non-condensable gas. Initially, the tank is filled with water at 30 °C. The nitrogen volume is modelled with non-condensable gas. For venting, the top of the tank is connected to a point, which is constantly at ambient pressure.

4.3 Pressurizer

As pressurizers, bladder accumulators are used, which contain a membrane separating the stored water volume from a nitrogen volume. As the code does not support changing volumes, no standard component could be used for modeling. For this reason, the actual pressure in the numerical model is calculated by the amount of coolant that is entering or leaving the pressurizer. Then, the resulting pressure is permanently passed as a boundary condition to a point resembling the accumulator.

Applying the ideal gas correlation, the gas pressure can be calculated as a function of the stored water inventory. The accumulator has a total inner volume of 54 dm^3. An operating pressure of 25 MPa results in a water inventory of 30 dm^3. A gas volume of 18.75 dm^3 corresponds to the maximum allowed pressure of 32 MPa. Thus, the pressure p [MPa] depends on the liquid mass m [kg] as:

$$p(m) = 1.4908E\text{-}05m^4 - 5.7743E\text{-}04m^3 + 1.4462E\text{-}02m^2 + 1.4885E\text{-}01m + 1.1154E+01.$$

The APROS model of such a pressurizer is shown in Figure 3. An additional shut of valve is needed in the model to prevent further outflow of coolant in case the accumulator got empty.

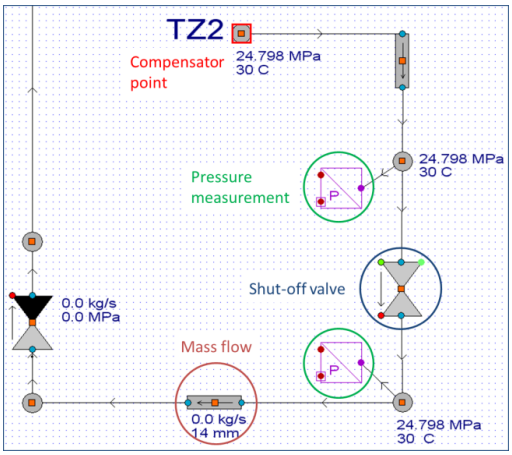

Fig 3. APROS model of a passive bladder accumulator.

5. Simulation of an automatic depressurization with long-term residual heat removal

In order to test the long-term coolability of the fuel rods, an automatic depressurization transient is simulated. The resulting temperature and pressure progress at the outlet of the test section is shown on the left-hand side of Figure 4.

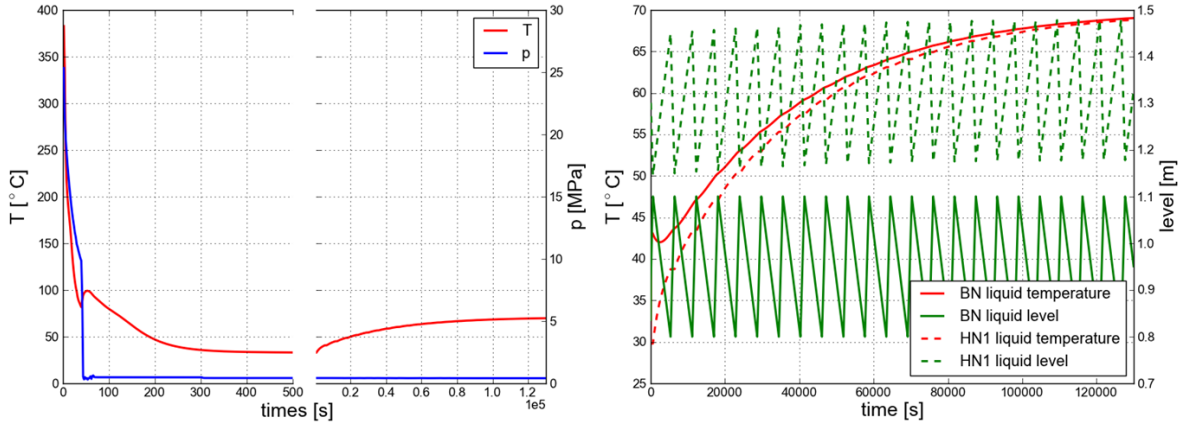

Fig 4. Pressure and temperature progress at the test section outlet (left) and liquid level and temperatures of the tanks (right) during a depressurization transient.

After 2 seconds, the reactor SCRAM gets activated and the reactor is depressurized over the ADS2 valve. 27 seconds after the beginning of the accident, the pressure in the primary circuit falls below 12 MPa and pump HC1 starts to inject into the feed-water line. The coolant temperature at the upper end of the fuel rods falls below 50 °C after 188 seconds and the fuel rods are well cooled for the complete simulation time of 130000 seconds. The right-hand side of Figure 4 depicts coolant level and temperature of the depressurization and coolant reservoir tank. As soon as the liquid level inside the depressurization tank (BN) reaches the upper limitation value of 1.1 m, coolant is automatically transferred back to the reservoir tank HN1 via the connecting line and pump HC3. The pump is stopped again in case the liquid level falls below the lower limit of 0.8 m. By this procedure, a closed coolant circuit is created which allows long-term residual heat removal. Furthermore, it is necessary to keep the secondary circuit running to serve as heat sink, where the inlet temperature on the secondary side of the U-tube cooler is fixed to 60 °C.

6. Conclusion and outlook

In the SCWR-FQT project, the commercial system code APROS is applied apart from its common use. Several parts and components of the loop could not be modeled by given standard components of the code. This paper presented how these components could be modeled alternatively with basic elements of the code. By employing the resulting numerical model, numerous accident analyses could be simulated. Thus, the model is a powerful tool supporting the design process of the loop with the final objective to license the test facility.

7. Acknowledgement

This work has been funded by the European Commission as part of their project SCWR-FQT, contract number 269908.

8. References

[1] www.hplwr.eu
[2] RAQUÉ, M., VOJACEK, A., HAJEK, P., SCHULENBERG, T.: Design and 1D Analysis of the Safety Systems for the SCWR Fuel Qualification Test, NUTHOS 9, Paper No. 124, Kaohsiung, Taiwan, 2012.
[3] APROS Version 5.08 / 5.09, VTT Finland and Fortum, http://APROS.vtt.fi/
[4] KURKI, J.: Simulation of thermal hydraulics at supercritical pressures with APROS, Thesis for the degree of Master of Science in Technology, Helsinki University of Technology, Department of Engineering Physics and Mathematics, 2008.
[5] HÄNNINEN, M., YLIJOKI, J.: The Constitutive Equations of the APROS Six-Equation Model, Manual in APROS Version 5.08, 2007.
[6] MOODY, F.: Maximum flow rate of a single component, two-phase mixture, Transactions of ASME, Journal of Heat Transfer, 86, pp. 134-142, 1965.

European Nuclear Society
Rue Belliard 65
1040 Brussels, Belgium
Telephone: +32 2 505 30 50 - FAX: +32 2 502 39 02
enc2012@euronuclear.org
www.enc-2012.org